6.02
Controls of Trace Metals in Seawater

K. W. Bruland and M. C. Lohan
University of California at Santa Cruz, CA, USA

6.02.1 INTRODUCTION

Since the early 1970s, marine chemists have gained a first-order understanding of the concentrations, distributions, and chemical behaviors of trace metals in seawater. Important factors initiating this quantum leap in knowledge were major advances in modern analytical chemistry and instrumentation, along with the development and adoption of clean techniques. An instrumental development in the mid-1970s that spurred the early research on trace metals was the availability of the sensitive graphite furnace as the sample introduction system to an atomic absorption spectrometer. More recently, the appearance of inductively coupled plasma (ICP) mass spectrometers has provided an even more sensitive and powerful instrumental capability to the arsenal of marine chemists. In addition to these instruments back in shore-based laboratories, there has been the development of sensitive shipboard methods such as stripping voltammetry and flow injection analysis (FIA) systems with either chemiluminescence or catalytically enhanced spectrophotometric detection. Along with the development of these highly sensitive analytical techniques came a recognition and appreciation of the importance of handling contamination issues by using clean techniques during all phases of sampling and analysis. This is necessary due to low concentrations of trace metals in seawater relative to the ubiquitousness of metals on a ship or in a laboratory (e.g., dust, steel hydrowire, rust, paint with copper and zinc antifouling agents, brass fittings, galvanized material, sacrificial zinc anodes, etc.). As a result, seawater concentrations of most trace metals have now been accurately determined in at least some parts of the oceans, and their oceanic distributions have been found to be consistent with oceanographic processes.

The concentrations and distributions of trace metals in seawater are controlled by a combination of processes. These processes include external sources of trace metals delivered by rivers along ocean boundaries, by wind-blown dust from arid and semi-arid regions of the continents, and by hydrothermal circulation at mid-ocean ridges. Processes removing trace metals from seawater include active biological uptake or passive scavenging onto either living or nonliving particulate material. Much of this particulate material (along with its associated trace metals) is internally recycled either in the water column or in surficial sediments. The ultimate sink of trace metals is generally marine sediments. These various sources and sinks are superimposed on the general circulation and mixing of the oceans, resulting in the characteristic distributions of each trace metal. One of the first examples of the emergence of oceanographically consistent vertical profiles was for the trace-metal cadmium (Boyle *et al*., 1976; Martin *et al*., 1976; Bruland *et al*., 1978a). These studies demonstrated that the distribution of dissolved cadmium in the sea follows a pattern similar to that of the nutrients phosphate and nitrate. Sparked by these surprising results, several investigators during the following two decades were able to obtain excellent data sets on a wide variety of trace metals. This chapter will attempt to provide a basic overview of what is known about the controls of the concentrations and distributions of trace metals in the open ocean. Subtleties in their distributions will not be presented. The distributions of trace metals in coastal regions are more dynamic and complicated and will not be discussed in this chapter.

The bulk of the data for vertical profiles of trace metals in seawater are from papers published in the 1980s and 1990s and most of the profiles are from either the North Pacific or North Atlantic. There is a paucity of vertical profiles from the South Atlantic and South Pacific. It has recently been argued that a new "GEOSECS"-type trace-metal program needs to be in place in order to provide appropriate global coverage of trace metals. Much of the impetus for such a program comes from the recognition of iron as an important micronutrient influencing global biogeochemical cycles in the oceans (Moore *et al*., 2002) and the potential role of other trace metals such as zinc. In particular, there is a pressing need for an expansion of the global database of dissolved iron distributions in the oceans. These measurements are needed to both initiate and verify models and to identify processes not contained in existing models.

There have been a number of reviews of trace elements in seawater that form a foundation for this chapter. Among them are: Bruland (1983) on oceanographically consistent data sets; Burton and Statham (1990) on trace metals in seawater; and Donat and Bruland (1995) on trace elements in oceans. There are two reviews that deal with more of the biological role of trace metals: Bruland *et al.* (1991) on interactive influence of bioactive trace metals on biological production in ocean waters; and Hunter *et al.* (1997) on biological roles of trace metals in natural waters. A highly complementary chapter in this Treatise that deals with the influence of essential trace metals on biological processes has been written by Morel *et al.* (Chapter 6.05). Turning to "on-line" sources of information, Nozaki has done an excellent job perusing the available literature and compiling vertical profiles from the North Pacific for each element in a periodic table that makes an excellent figure (http://www.agu.org/eos_elec/97025e.html). Ken Johnson, a marine chemist at the Monterey Bay Aquarium Research Institute (MBARI), has a web site with a periodic table of the elements containing a brief review of information on each element (http://www.mbari.org/chemsensor/pteo.htm).

6.02.1.1 Concentrations

Concentrations of trace metals in seawater fall within a range bounded by ~10 μmol kg^{-1} at the upper end and extending through fmol kg^{-1} at the lower end (μ(micro) $= 10^{-6}$, n (nano) $= 10^{-9}$, p (pico) $= 10^{-12}$, and f (fempto) $= 10^{-15}$). The concentrations of metals in seawater range over 15 orders of magnitude from sodium, the most abundant cation, at a concentration close to 0.5 mol kg^{-1} to iridium at a concentration as low as 0.5 fmol kg^{-1}. A concentration of 10 μmol kg^{-1} (~1 ppm by weight) is chosen as the concentration separating trace metals from the major and minor metals in seawater. The mean concentration of a trace metal is strongly influenced by its deep-water value, particularly that found in the deep waters of the Pacific Ocean with its large volume. Table 1 presents the range of concentrations and their mean for many of the elements in seawater along with an estimate of the major inorganic form or species found in seawater.

Trace metals in seawater can exist in a variety of physical and chemical forms. The simplest physical distinction is particulate versus dissolved forms. This is somewhat of an operational definition with 0.4 μm or 0.2 μm pore size filters generally providing this separation. Particulate forms include those metals adsorbed onto particle surfaces, incorporated within particles of biogenic origin and incorporated in the matrix of aluminosilicate minerals or co-precipitated in other authigenic minerals. Dissolved metals include various soluble complexes of the trace metals and potential colloidal forms. The redox chemistry of the particular metal and its environment dictate the oxidation state and form of the parent species. For trace metals, the parent species can be the simple mono-, di-, or trivalent cation such as Zn^{2+}, or for metals existing in higher

Table 1 A periodic table of the elements in seawater indicating the element number, the dominant inorganic species predicted to be found in the oceans, the range of concentrations observed in the open ocean, and an estimate of the element's mean concentration. The mean concentration is shown on the left-hand column in parenthesis and on the right-hand column as a thick line. Hydrogen, noble gases, lanthanides, and elements after lead are omitted.

3	Li	Li^+	*(25.9 μmol kg^{-1})*
4	Be	$Be(OH)^+$, $Be(OH)_2^0$	4 to 30 pmol kg^{-1} *(23)*
5	B	H_3BO_3	*(416 μmol kg^{-1})*
6	C	HCO_3^-	1.9 to 2.5 mmol kg^{-1} *(2.25)*
7	N	N_2	350 to 610 μmol kg^{-1} *(590)*
7	N	NO_3^-	0.01 to 45 μmol kg^{-1} *(30)*
8	O	O_2	1 to 350 μmol kg^{-1} *(175)*
9	F	F^-	*(68 μmol kg^{-1})*
11	Na	Na^+	*(468 mmol kg^{-1})*
12	Mg	Mg^{2+}	*(53 mmol kg^{-1})*
13	Al	$Al(OH)_4^-$, $Al(OH)_3^0$	0.3 to 40 nmol kg^{-1} *(~2)*
14	Si	H_4SiO_4	0.5 to 180 μmol kg^{-1} *(100)*
15	P	HPO_4^{2-}	0.001 to 3.5 μmol kg^{-1} *(2.3)*
16	S	SO_4^{2-}	*(28 mmol kg^{-1})*
17	Cl	Cl^-	*(546 mmol kg^{-1})*
19	K	K^+	*(10.2 mmol kg^{-1})*
20	Ca	Ca^{2+}	10.1 to 10.3 mmol kg^{-1} *(10.3)*
21	Sc	$Sc(OH)_3^0$	8 to 20 pmol kg^{-1} *(16)*
22	Ti	$Ti(OH)_4^0$, $TiO(OH)_2^0$	6 to 250 pmol kg^{-1} *(160)*
23	V	HVO_4^{2-}	30 to 36 nmol kg^{-1}
24	Cr	CrO_4^{2-}	3 to 5 nmol kg^{-1} *(4)*
25	Mn	Mn^{2+}	0.08 to 5 nmol kg^{-1} *(0.3)*
26	Fe	$Fe(OH)_2^+$, $Fe(OH)_3^0$	0.02 to 2 nmol kg^{-1} *(0.5)*
27	Co	Co^{2+}	4 to 300 pmol kg^{-1} *(20)*
28	Ni	Ni^{2+}	2 to 12 nmol kg^{-1} *(8)*
29	Cu	$CuCO_3^0$	0.5 to 4.5 nmol kg^{-1} *(3)*
30	Zn	Zn^{2+}	0.05 to 9 nmol kg^{-1} *(5)*
31	Ga	$Ga(OH)_4^-$	12 to 30 pmol kg^{-1}
32	Ge	H_4GeO_4	1 to 100 pmol kg^{-1} *(70)*
32	Ge	MethylGe	*(400 pmol kg^{-1})*
33	As	$HAsO_4^{2-}$	20 to 25 nmol kg^{-1} *(23)*
34	Se	SeO_4^{2-}	0.5 to 2.3 nmol kg^{-1} *(1.7)*
35	Br	Br^-	*(0.84 mmol kg^{-1})*

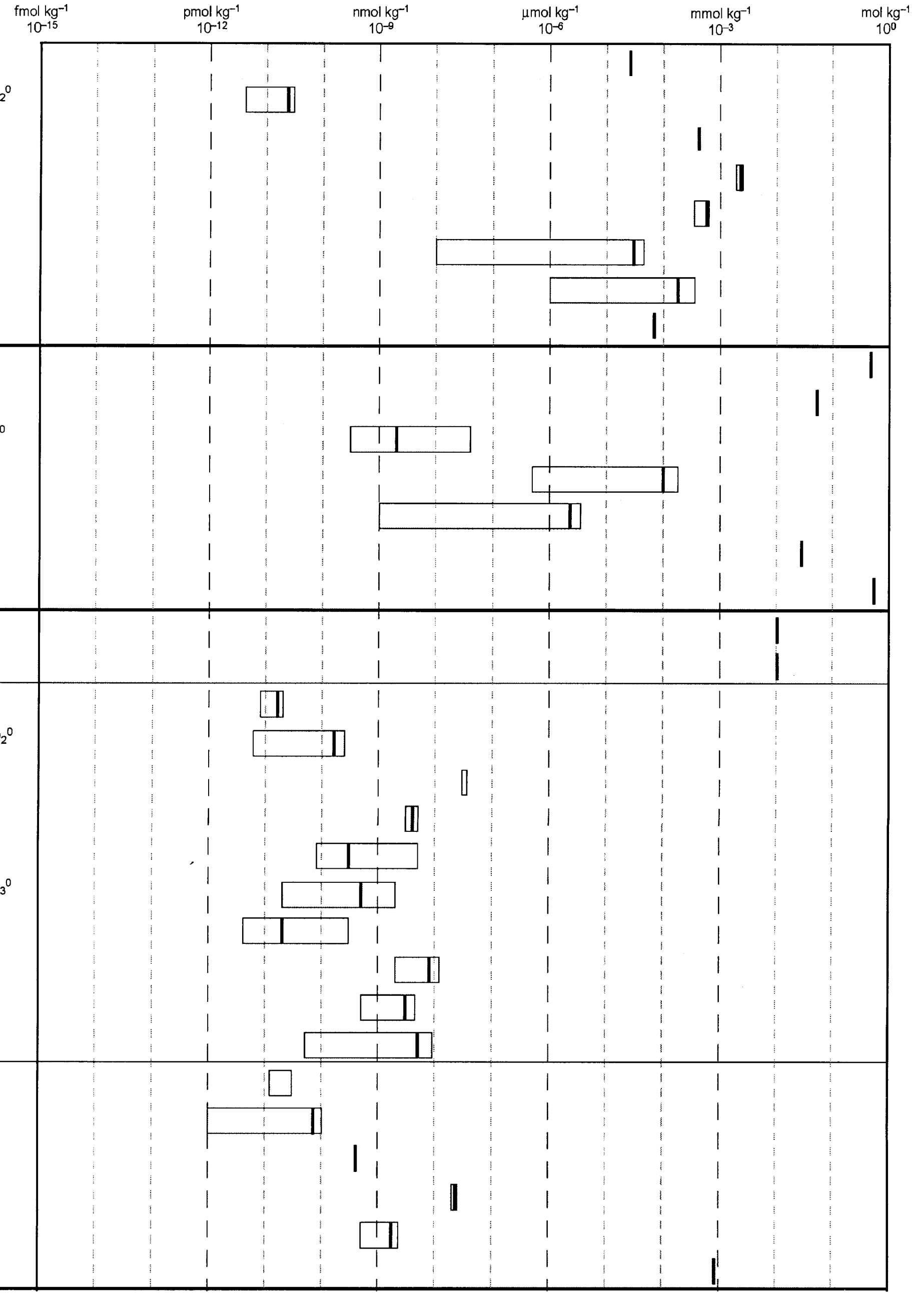

(continued)

Table 1 (continued).

37	**Rb**	Rb$^+$	*(1.4 μmol kg^{-1})*
38	**Sr**	Sr^{2+}	*(90 μmol kg^{-1})*
39	**Y**	Y(CO$_3$)$^+$, Y(OH)$^{2+}$	60 to 300 pmol kg^{-1} *(200)*
40	**Zr**	Zr(OH)$_5^-$, Zr(OH)$_4^0$	12 to 300 pmol kg^{-1} *(200)*
41	**Nb**	Nb(OH)$_6^-$, Nb(OH)$_5^0$	≤50 pmol kg^{-1}
42	**Mo**	MoO$_4^{2-}$	*(105 nmol kg^{-1})*
43	**Tc**		No stable isotope
44	**Ru**	Ru(OH)$_n^{4-n}$	< 50 fmol kg^{-1} ?
45	**Rh**	Rh(OH)$_n^{3-n}$, RhCl$_n^{3-n}$	0.4 to 1 pmol kg^{-1} *(0.8)*
46	**Pd**	PdCl$_4^{2-}$	0.2 to 0.7 pmol kg^{-1} *(0.6)*
47	**Ag**	AgCl$_2^-$, AgCl$_3^{2-}$	1 to 35 pmol kg^{-1} *(20)*
48	**Cd**	CdCl$_2^0$	1 to 1000 pmol kg^{-1} *(600)*
49	**In**	In(OH)$_3^0$	40 to 100 fmol kg^{-1} *(70)*
50	**Sn**	SnO(OH)$_3^-$, Sn(OH)$_4^0$	1 to 20 pmol kg^{-1} *(4)* ?
51	**Sb**	Sb(OH)$_6^-$	*(1.6 nmol kg^{-1})*
52	**Te**	Te(OH)$_6^0$	0.5 to 1.2 pmol kg^{-1} *(0.6)*
53	**I**	IO$_3^-$	400 to 460 nmol kg^{-1} *(450)*
55	**Cs**	Cs$^+$	*(2.2 nmol kg^{-1})*
56	**Ba**	Ba^{2+}	30 to 150 nmol kg^{-1} *(110)*
57–71	Lanthanides		
71	**Lu**	Lu(CO$_3$)$^+$, Lu(OH)$^{2+}$	0.3 to 1.5 pmol kg^{-1} *(1)*
72	**Hf**	Hf(OH)$_4^0$, Hf(OH)$_5^-$	100 to 800 fmol kg^{-1} *(700)*
73	**Ta**	Ta(OH)$_5^0$	60 to 220 fmol kg^{-1} *(200)*
74	**W**	WO$_4^{2-}$	*(60 pmol kg^{-1})*
75	**Re**	ReO$_4^-$	*(40 pmol kg^{-1})*
76	**Os**	H$_3$OsO$_6^-$	15 to 60 fmol kg^{-1} *(50)* ?
77	**Ir**	Ir(OH)$_3^0$?	0.5 to 1 fmol kg^{-1}
78	**Pt**	PtCl$_4^{2-}$?	0.2 to 1.5 pmol kg^{-1} *(0.25)* ?
79	**Au**	AuCl$_2^-$?, Au(OH)$_3^0$?	10 to 100 fmol kg^{-1} *(<100)*
80	**Hg**	HgCl$_4^{2-}$	0.2 to 2 or 2 to 10 pmol kg^{-1} ? *(1)*?
81	**Tl**	Tl$^+$, TlCl^0	60 to 80 pmol kg^{-1} *(70)*
82	**Pb**	PbCO$_3^0$	5 to 150 pmol kg^{-1} *(10)*

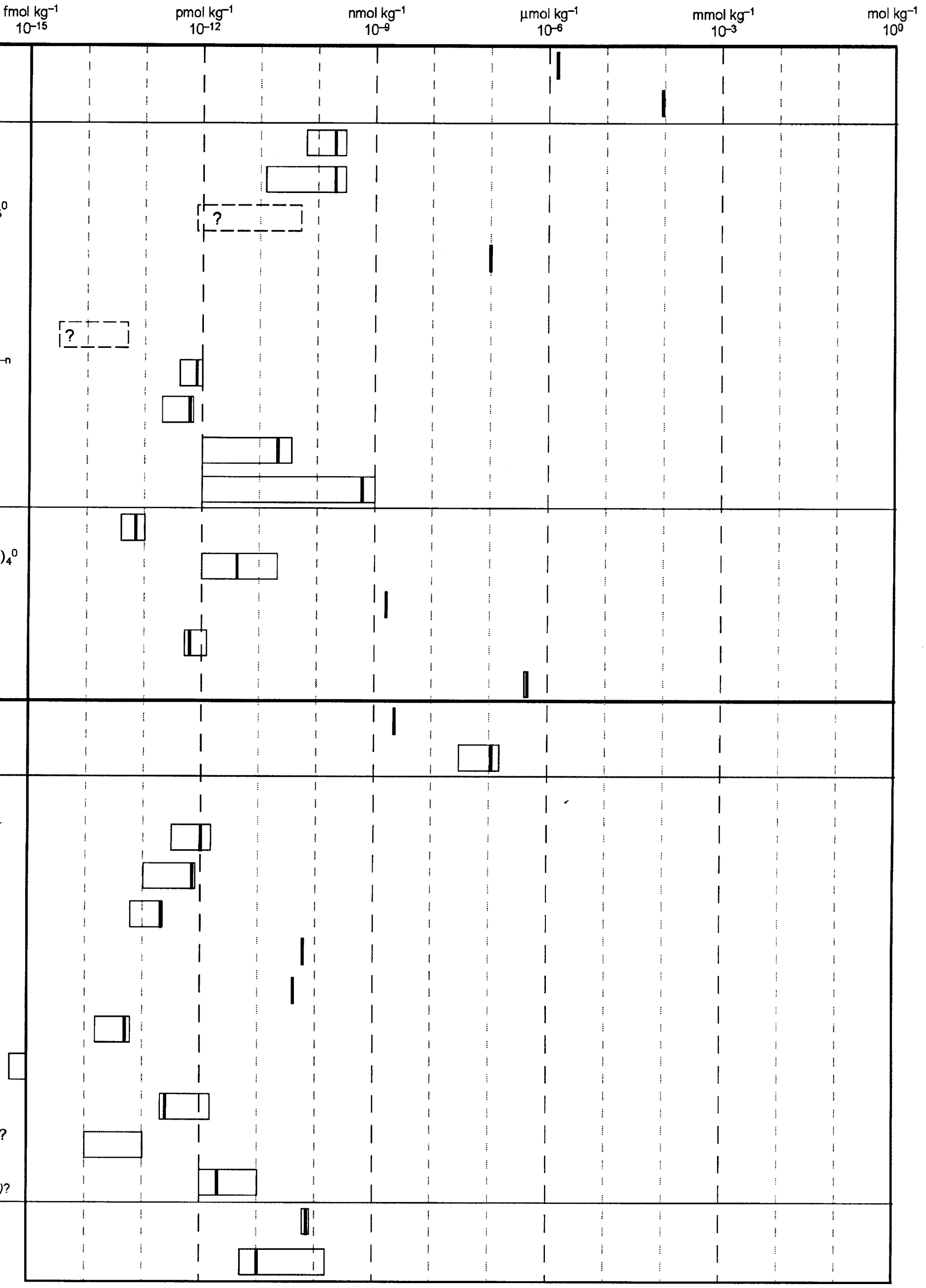

oxidation states, it can be an oxycation such as UO_2^{2+} or an oxyanion such as MoO_4^{2-}. For a trace metal such as mercury, the parent species can be Hg^{2+}, CH_3Hg^+, or Hg^0. Cationic parent species can form complexes with a variety of both inorganic and organic ligands in seawater. For example, Hg^{2+} will complex with chloride and exist primarily as $Hg(Cl)_4^{2-}$, and UO_2^{2+} will complex with carbonate and exist as the uranyl carbonate complex $(UO_2(CO_3)_3^{4-})$.

The inorganic speciation presented in Table 1 is primarily taken from the compilations of Turner *et al.* (1981) and Byrne *et al.* (1988). Turner *et al.* (1981) used a database of stability constants for more than 500 metal complexes to calculate the inorganic speciation for 58 trace elements in model seawater at pH 8.2, 25 °C, and 1 atm. Byrne *et al.* (1988) extended this work by considering the influence of temperature and pH on speciation. The free hydrated divalent cation dominates the dissolved inorganic speciation of Zn(II) and the first transition series metals Mn(II), Co(II), and Ni(II). Strongly hydrolyzed trace metals include Be(II), Al(III), Fe(III), and Ga(III). Trace metals whose dissolved speciation is dominated by chloride complexation include Cd(II), Hg(II), Ag(I), and Pd(II).

The complexation or chelation of trace metals with organic ligands will be discussed separately at the end of this chapter. As we will see, the chemistry and behavior of many trace metals in the water column is dominated by complexation, biological assimilation at uptake sites on cell surfaces, and adsorption on surface sites of suspended particles. All three of these processes, which are particularly important in surface waters where biological activity is most intense, are controlled by similar coordination mechanisms (Hering and Morel, 1990).

Starting at the beginning of the periodic table, beryllium (element #4) is the first trace metal, and is the only trace metal with an atomic number less than 12. Beryllium has a concentration range in the oceans of 4–30 pmol kg^{-1} (Measures and Edmond, 1982) and exists as Be(II) with the hydrolysis species $Be(OH)^+$ and $Be(OH)_2^0$ as the major inorganic species. Aluminum (element #13) is the next trace metal encountered in the periodic table. Although aluminum is very abundant in the Earth's crust, it is a trace metal in the open ocean with concentrations ranging between 0.3 nmol kg^{-1} and 40 nmol kg^{-1} (Hydes, 1983; Orians and Bruland, 1986). Dissolved aluminum exists as Al(III), with the hydrolysis species $Al(OH)_3^0$ and $Al(OH)_4^-$ dominating its inorganic speciation.

All of the first-row transition metals are trace metals with concentrations ranging by a factor of 10^4—from a low of 4 pmol kg^{-1} up to 36 nmol kg^{-1}. The least abundant first-row transition metal is cobalt, thought to exist as Co(II), with a concentration range of 4–300 pmol kg^{-1}, while the most abundant is vanadium, existing as the vanadate oxyanion (HVO_4^{2-}) at a concentration between 30 nmol kg^{-1} and 36 nmol kg^{-1}. Interestingly, the most abundant transition metal in the oceans is molybdenum (element #42), existing at ~105 nmol kg^{-1} (Sohrin *et al.*, 1989) as Mo(VI) in the form of the molybdate oxyanion (MoO_4^{2-}). The least abundant trace metal in seawater (excluding radioactive elements) is thought to be the platinum group metal iridium (element #77). Iridium is extremely rare in the Earth's crust and its seawater concentration is reported to be between 0.5 fmol kg^{-1} and 1 fmol kg^{-1} (Anbar *et al.*, 1996). It is thought to exist as Ir(III) primarily as the hydrolysis species $Ir(OH)_3^0$. The analytical challenges of determining the concentration of an element at sub-femptomolar concentrations ($<10^{-15}$ M) are impressive indeed. In this case it was determined by isotope dilution using thermal ionization mass spectrometry after concentration with anion exchange resins.

6.02.1.2 Distributions

Trace metals exhibiting a relatively narrow range of concentrations in seawater tend to exist either as oxyanions (MoO_4^{2-}, WO_4^{2-}, ReO_4^{2-}) or as larger monovalent cations (Cs^+, Rb^+). Some of these metals such as molybdenum have a significant biological requirement; however, they tend to exist in seawater at relatively high concentrations relative to their requirement by the biota. Those trace metals exhibiting the greatest range in concentrations tend to be intimately involved in the major biogeochemical cycles and are actively assimilated by phytoplankton in surface waters. These include trace metals such as iron, zinc, and cadmium. Trace metals have been grouped into three principal categories reflecting their distributions and chemical behavior in seawater: conservative, nutrient, and scavenged.

6.02.1.2.1 Conservative-type distributions

Conservative-type trace metals interact only weakly with particles, have oceanic residence times greater than 10^5 yr (much greater than the mixing time of the oceans), and have concentrations that maintain a relatively constant ratio to salinity. Trace metals with conservative-type distributions in seawater such as molybdenum, antimony, tungsten, rhenium, caesium, and rubidium are involved in the major biogeochemical cycles of particle formation and destruction, but this is negligible relative to their concentration in seawater. Molybdenum is probably the best example of a conservative-type trace metal. It exists at an average concentration of 105 nmol kg^{-1} as the oxyanion molybdate, MoO_4^{2-}, and has an oceanic residence time of $\sim 8 \times 10^5$ yr (Emerson and Huested, 1991). It exhibits an almost uniform distribution in the oceans with only a slight depletion at the surface. Although molybdenum is required as an essential metal co-factor in a number of enzymes such as nitrogenase, this requirement is small relative to the amount of molybdenum available and does not impact its distribution appreciably. In addition, negatively charged anions such as MoO_4^{2-} have a relatively low particle affinity at the slightly basic pH of seawater. Other trace metals existing as oxyanions that exhibit relatively conservative-type behavior include tungstate (WO_4^{2-}) and perrhenate (ReO_4^-).

There is interest in the use of some of these oxyanions as potential paleogeochemical proxies of the oxygen content or the redox state of deep waters (Emerson and Huested, 1991; Morford and Emerson, 1999). For example, under anoxic conditions molybdenum can be reduced from the +6 oxidation state as an oxyanion to insoluble $MoS_2(s)$ or converted to particle-reactive thiomolybdates (Vorlick and Helz, 2002).

Other examples of conservative-type trace metals include caesium and rubidium. Caesium(I) exists at an average concentration of 2.2 nmol kg^{-1} (Brewer *et al.*, 1972) as the relatively unreactive monovalent cation Cs^+. Its oceanic residence time has been estimated to be ~3 × 10^5 yr (Broecker and Peng, 1982). Rubidium exists as the monovalent cation Rb^+ at a concentration of 1.4 μmol kg^{-1} (Spencer *et al.*, 1970) with an oceanic residence time estimated to be 3 Myr.

6.02.1.2.2 Nutrient-type distributions

Trace metals with nutrient-type distributions are significantly involved with the internal cycles of biologically derived particulate material. Their distributions are dominated by the internal cycle of assimilation by plankton in surface waters and the export production or transport of part of this material out of the surface layer followed by oxidation and remineralization of the bulk of this material in deeper waters. Consequently, their concentrations are lowest in surface waters where they are assimilated by phytoplankton and/or adsorbed by biogenic particles, and increase in the subsurface waters as sinking particles undergo decomposition or dissolution. In addition, nutrient-type metals exhibit a relatively low level of scavenging in the deep sea and thus their concentrations increase along the flow path of water in the world's oceans as the water ages. Oceanic residence times of nutrient-type, recycled elements are intermediate (a few thousand to one hundred thousand years).

Zinc is perhaps the most striking example of a trace metal with a nutrient-type distribution in the oceans. Bruland *et al.* (1978b) reported the first accurate zinc distribution in seawater and demonstrated its strong correlation with silicic acid. Subsequently, Bruland (1980), Bruland and Franks (1983), Martin *et al.* (1989, 1993), Morley *et al.* (1993), Bruland *et al.* (1994), and Lohan *et al.* (2002) have provided other consistent profiles. Characteristic vertical profiles of dissolved zinc and silicic acid from high latitudes of the North Atlantic and North Pacific are presented in Figure 1, demonstrating the strong interbasin fractionation that exists for this nutrient-type trace metal. The concentration data available for deep waters of the oceans yield a linear relationship between dissolved zinc (nmol kg^{-1}) and silicic acid (μmol kg^{-1}): $[Zn] = 0.05[H_4SiO_4] + 0.8$. Figure 2(a) presents the distribution of silicic acid at 3,000 m depth in the world's oceans (from the NODC data set) and, using the above relationship between silicic acid and dissolved zinc, Figure 2(b) illustrates the estimated dissolved zinc concentration at 3,000 m depth. Silicic acid increases by a factor of 10 from a concentration of 20 μmol kg^{-1} at a depth of 3,000 m at high latitudes of the North Atlantic to 200 μmol kg^{-1} at high latitudes of the North Pacific. Similarly, dissolved zinc increases by a factor of 5 from 2 nmol kg^{-1} in the young waters of the western North Atlantic to 10 nmol kg^{-1} in

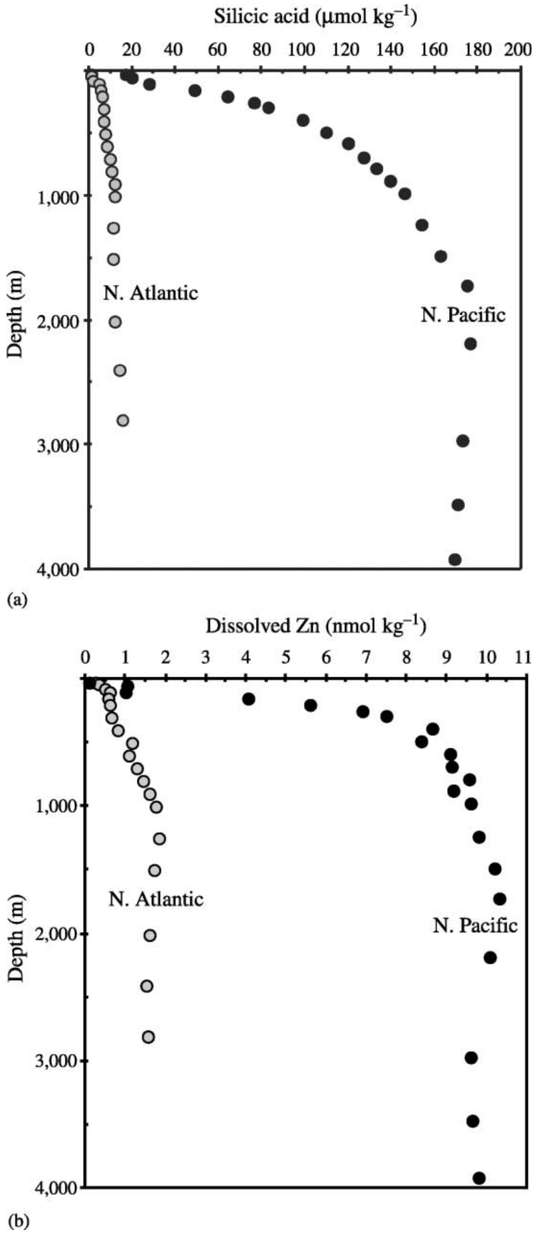

Figure 1 Vertical profiles of (a) silicic acid and (b) dissolved zinc observed at high latitudes of the North Atlantic (○) (59° 30′ N, 20° 45′ W; data from Martin *et al.*, 1993) and the North Pacific (●) (50° N, 145° W; data from Martin *et al.*, 1989).

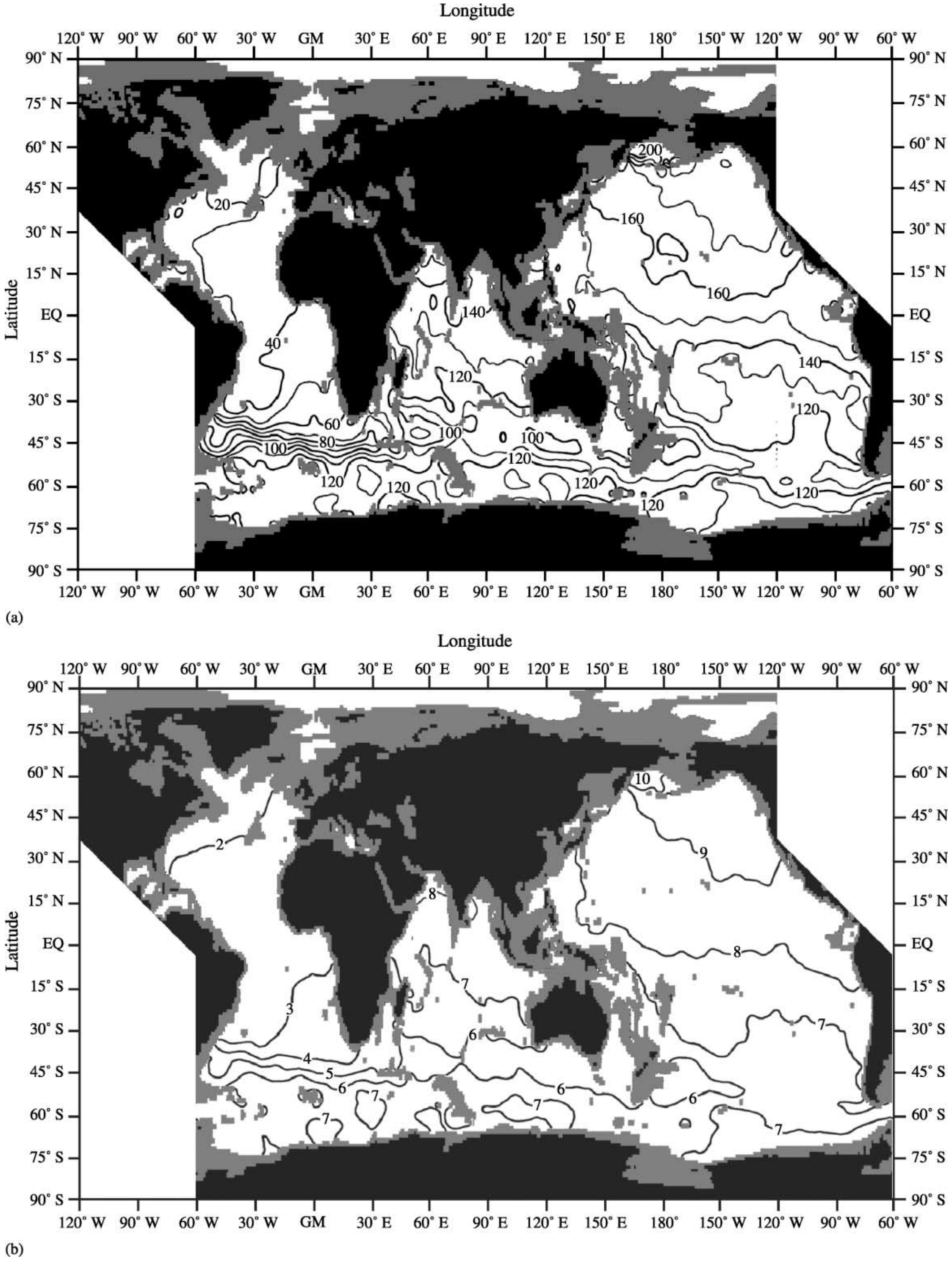

Figure 2 Horizontal gradients of the annual mean concentration of (a) silicic acid (μmol kg^{-1}) at 3,000 m depth in the world's oceans (source NODC), and (b) dissolved zinc (nmol kg^{-1}) at a depth of 3,000 m based upon the deep-water relationship ($[Zn] = 0.05[H_4SiO_4] + 0.8$) between silicic acid and dissolved zinc from stations in the North Atlantic (Bruland and Franks, 1983; Martin *et al*., 1993), North Pacific (Bruland, 1980; Martin *et al*., 1989; Bruland *et al*., 1994), and Southern Ocean (Martin *et al*., 1990).

the old deep waters found at high latitudes of the North Pacific. Similar figures can be produced for the nutrient-type trace metal cadmium using the strong correlation between cadmium and phosphate or nitrate in deep waters of the oceans. Barium also exhibits a nutrient-type distribution with concentrations ranging from 35 nmol kg^{-1} in surface waters to 56 nmol kg^{-1} at 3,000 m depth in the North Atlantic, and increasing along the flow path of deep water to concentrations of 150 nmol kg^{-1} in the deep North Pacific (Chan *et al.*, 1976, 1977).

Silver provides another interesting example of a nutrient-type trace metal with a strong interbasin fractionation. The first accurate data were reported by Martin *et al.* (1983) for the eastern North Pacific where they observed values of 0.4 pmol kg^{-1} in surface waters increasing to 23 pmol kg^{-1} at a depth of 2,300 m. Figure 3 presents dissolved silver depth profiles from high latitudes of the North Atlantic (Rivera-Duarte *et al.*, 1999) and high latitudes of the Northwest Pacific (Zhang *et al.*, 2001). Vertical profiles of dissolved silver exhibit a strong similarity to silicic acid and the deep waters of the Northwest Pacific are enriched by slightly more than a factor of 10 for silicic acid and slightly less than a factor of 10 for silver (Figure 3). This interbasin fractionation for silver represents an even greater fractionation than that observed for zinc. It is unclear why silver would exhibit such a nutrient-type profile, since there is no known biological requirement for silver. Perhaps the nutrient metal acquisition sites are not selective enough to discriminate against silver and it is mistakenly assimilated into phytoplankton by the zinc (or some other metal) uptake system. Alternatively, silver may be passively adsorbed to selected surface sites of biogenic particles and transported to depth where it is remineralized as the biogenic particulate material undergoes oxidation or dissolution. Nutrient-type trace metals have been used as paleoproxies for nutrient concentrations or ages of deep waters in the geologic past. Good direct fossil records of the phosphate, nitrate, or silicic acid content of deep waters do not exist. Thus, the fossil record of nutrient-type trace metals such as cadmium or zinc whose concentrations mimic and are strongly correlated with the macronutrients phosphate, nitrate, or silicic acid, can serve as indirect proxies of past nutrient conditions. The best known example involves the use of cadmium (Boyle, 1988), where the Cd/Ca ratio in benthic foraminifera in sediment cores can be used to infer the past concentrations of cadmium in deep seawater, and by correlation, phosphate in the overlying deep waters. This approach is complementary to the use of more standard tracers such as δ^{13}C. The nutrient-type distribution of zinc has also been used as a paleoproxy for the age and nutrient content of deep waters (Marchitto *et al.*, 2002). These researchers used increases in benthic foraminiferal Zn/Ca and Cd/Ca ratios as evidence for a greatly increased presence of nutrient-rich Southern Ocean water in the glacial North Atlantic versus relatively nutrient-poor North Atlantic deep water.

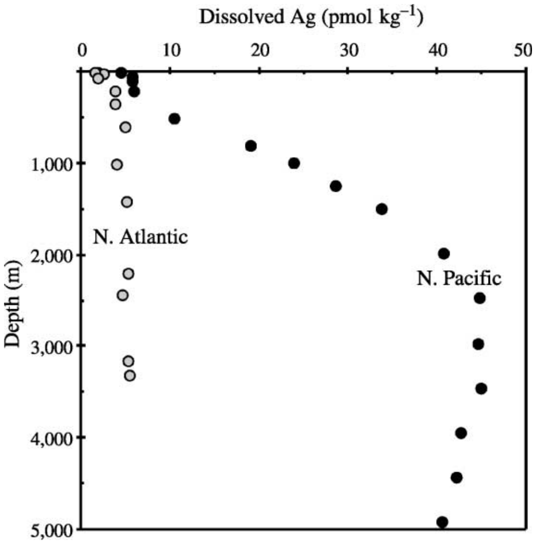

Figure 3 Vertical profiles of dissolved silver in the North Atlantic (○) (composite of two stations 54.5° N, 48.5° W, and 52.7° N, 35° W; data from Rivera-Duarte *et al.*, 1999) and the western North Pacific (●) (40° N, 145° W; data from Zhang *et al.*, 2001).

6.02.1.2.3 *Scavenged-type distributions*

Trace metals with scavenged-type distributions have strong interactions with particles and short oceanic residence times (~100–1,000 yr), residence times that are less than the ventilation or mixing time of the oceans. Their concentrations tend to be maximal near major sources such as rivers, atmospheric dust, bottom sediments, and hydrothermal vents. Concentrations decrease with distance from the sources and, in general, the concentrations of the scavenged metals tend to decrease along the flow path of deep water due to continual particle scavenging.

Aluminum is the best illustration of a trace metal with a scavenged-type distribution in the oceans. The major external input of aluminum is from the partial dissolution of atmospheric dust delivered to the surface ocean. Vertical profiles in the Mediterranean, the North Atlantic, and the North Pacific are presented in Figure 4. Extremely elevated concentrations of dissolved aluminum are observed in the Mediterranean Sea (Hydes *et al.*, 1988), a region that receives a high atmospheric input of dust. Concentrations in

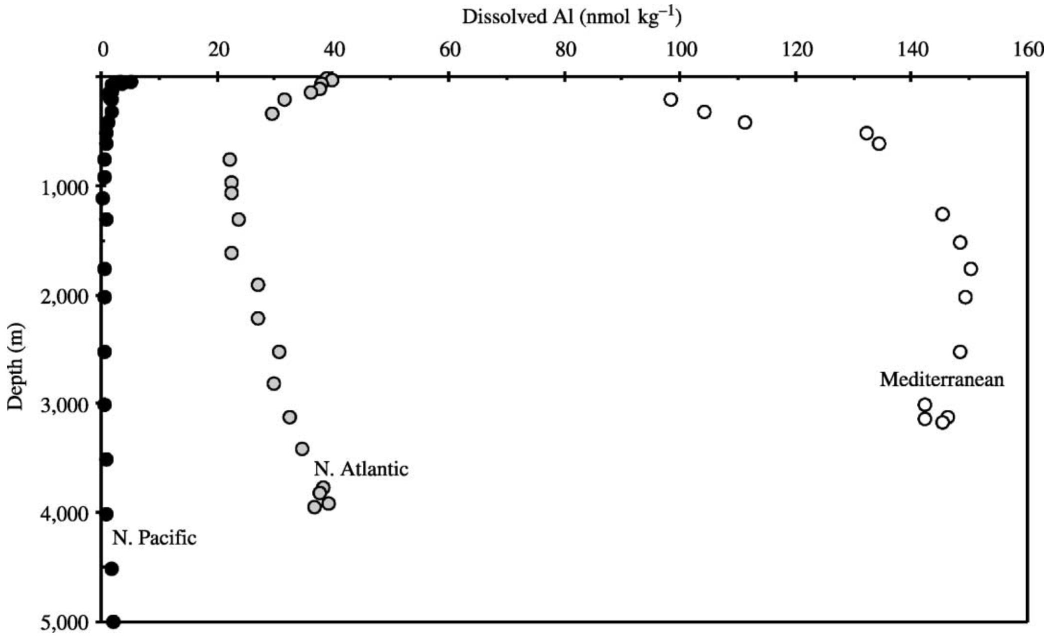

Figure 4 Vertical profiles of dissolved aluminum in the Mediterranean Sea (○) (34° 18′ N, 20° 02′ W; data from Hydes *et al.*, 1988), the North Atlantic (◉) (40° 51′ N, 64° 10′ W; data from Hydes, 1979), and the North Pacific (●) (28° 15′ N, 155° 07′ W; data from Orians and Bruland, 1986).

the North Atlantic (Hydes, 1983) are maximal in the surface waters and elevated throughout the relatively young deep waters of the North Atlantic. The surface waters of the North Pacific, a region that receive less dust input than the Atlantic, exhibit aluminum concentrations that are correspondingly lower (Orians and Bruland, 1985, 1986). The old deep waters of the North Pacific have dissolved aluminum concentrations that are (8–40)-fold lower than in the North Atlantic and ~100-fold lower than those observed in the Mediterranean. This decrease along the deep-water flow path is consistent with an oceanic residence time for dissolved aluminum of only ~200 yr (Orians and Bruland, 1986). This marked difference between the North Pacific and North Atlantic deep waters is the reverse of that shown by the nutrient-type trace metals and the greatest interbasin fractionation of any trace metal. Unfortunately, it does not appear that this marked interbasin fractionation observed for dissolved aluminum can be utilized as a paleogeochemical tracer.

6.02.1.2.4 *Hybrid distributions*

Some trace metals, such as iron and copper, have distributions that are strongly influenced by both recycling and relatively intense scavenging processes. Like nutrient-type elements, dissolved iron is observed to be depleted in remote oceanic surface waters such as high-nutrient, low-chlorophyll (HNLC) regimes, and appears to be regenerated with depth (Figure 5) (Martin and Gordon, 1988; Johnson *et al.*, 1997). In less productive waters of the oligotrophic central gyres, particularly in areas of high dust inputs, dissolved iron can exhibit surface-water maxima more indicative of scavenged elements (Bruland *et al.*, 1994; Measures *et al.*, 1995; Johnson *et al.*, 1997). While nutrient-type metals, with their relatively long oceanic

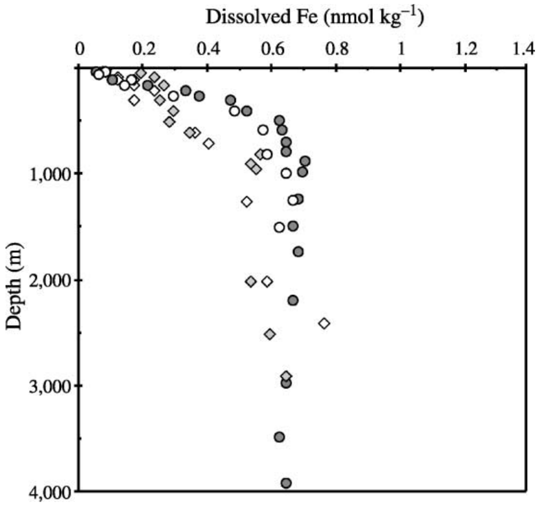

Figure 5 Vertical profiles of dissolved iron from high latitudes of the North Atlantic (◈, ◇) (59° 30′ N, 20° 45′ W and 47° N, 20° W; data from Martin *et al.*, 1993) and the North Pacific (◉, ○) (50° N, 145° W and 45° N, 142° 52′ W; data from Martin *et al.*, 1989).

residence times, tend to increase in concentration in the deep waters of the ocean as the latter age, the residence time of iron in deep waters is estimated to be ~200 yr and does not exhibit this trend. Figure 5 presents vertical profiles of dissolved iron in remote high-latitude regions of the North Atlantic and North Pacific oceans. The concentration of iron at depths greater than 1,000 m is not significantly different, which is in marked contrast to profiles of nutrients or nutrient-type trace metals. Instead, the deep-water concentration of dissolved iron appears to be controlled by a balance of remineralization from the rain of particulates from above and particulate scavenging (Johnson *et al*., 1997).

6.02.1.2.5 Mixed distributions

There are also trace metals that exist in more than one chemical form with substantially differing distributions. A fascinating example involves the trace element germanium. Germanium (element #32) is located just beneath silicon in the periodic table. Inorganic germanic acid behaves similar to silicic acid in seawater (Froelich and Andreae, 1981). It is assimilated at a molar ratio Ge : Si of ~0.7×10^{-6} into the siliceous tests of diatoms and other planktonic organisms that make tests of biogenic opal. When the tests dissolve, the germanium is released in the same ratio and as a result there is a tight correlation between the distribution of germanic acid (H_4GeO_4) and silicic acid (H_4SiO_4) in seawater (Froelich and Andreae, 1981). Unlike silicon, however, germanium is also found to exist as the methylated forms $CH_3Ge(OH)_3^0$ and $(CH_3)_2Ge(OH)_2^0$ (Lewis *et al*., 1989), that appear so stable to degradation that they have been called the "Teflon of the sea." The remarkable stability of these methylated species is reflected in their conservative vertical profiles (concentrations of dimethylgermanium are 100 pmol kg^{-1} and monomethylgermanium are 310–330 pmol kg^{-1}) (Figure 6). This conservative distribution is in marked contrast to the nutrient-type distribution of germanic acid (2–120 pmol kg^{-1}). There are a number of other examples of methylated compounds that comprise a significant fraction of trace metals and metalloids in seawater (e.g., arsenic, selenium, mercury, tin).

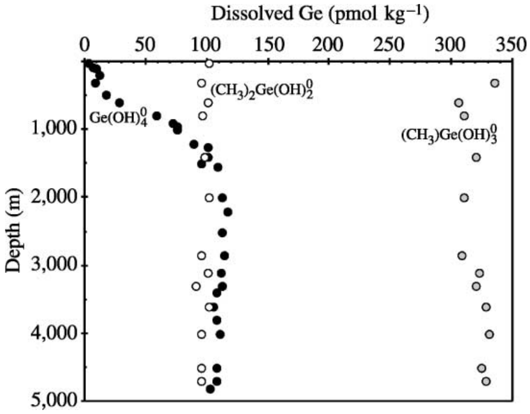

Figure 6 Vertical profiles of dissolved germanium species from the North Pacific: inorganic germanium (●) (25° N, 170° 05′ E; data from Froelich and Andreae, 1981); methyl-germanium (○, ○) (data from Lewis *et al*., 1985).

6.02.2 EXTERNAL INPUTS OF TRACE METALS TO THE OCEANS

6.02.2.1 Rivers

For the major ions in seawater, the input from rivers is generally the dominant source. The historical approach to estimate the river flux of major elements is to measure their concentrations in both dissolved and particulate forms in the river and multiply these concentrations by the river discharge rate, thus arriving at the input of both forms of the elements. For trace metals, however, estimating the river flux is more difficult. There are major problems due to under-sampling of representative river systems. Although large rivers dominate the global river input to the oceans, such rivers are located in remote regions and are insufficiently sampled to allow adequate fluxes of dissolved trace-metal concentrations in relation to season and flow to be determined (Jickells, 1995). Most of the historical river data for trace metals are not accurate, and the development of trace-metal clean techniques also needs to be applied to river sampling (Shiller and Boyle, 1991; Windom *et al*., 1991; Kim *et al*., 1999).

Not only are accurate data for trace metals in rivers sparse, there are complications that exist at the river–sea interface. The increase in salinity occurring at the river–sea water interface, with its concomitant increase in the concentrations of the major seawater cations, can lead to flocculation and sedimentation of trace metals such as iron (Boyle *et al*., 1978; Sholkovitz and Copeland, 1983) or to desorption from suspended riverine particles of trace metals such as barium (Edmond *et al*., 1978). In organic-rich rivers a major fraction of dissolved trace metals can exist in physiochemical association with colloidal humic acids. Sholkovitz and Copeland (1983) used "product-mode" mixing experiments on filtered Scottish river water, and observed that iron removal was almost complete due to the flocculation of strongly associated iron-humic acid colloids in the presence of the increased concentrations of Ca^{2+} and Mg^{2+} found in estuaries. Copper and nickel were also removed to an appreciable extent. This removal within estuarine mixing zones is not as important in rivers with lower dissolved organic carbon content. Nonconservative behavior within estuaries makes it difficult to obtain realistic estimates of the actual river input of trace metals to the oceans.

6.02.2.2 Atmosphere

Using a sparse network of field measurements of atmospheric aerosols, Duce and Tindale (1991) were able to provide some of the first global estimates of atmospheric dust input to the oceans. More recently, satellites have provided estimates of the global distribution of atmospheric aerosols allowing model estimates of dust deposition (Tegen and Fung, 1995; Mahowald *et al*., 1999). Figure 7 presents the results of such models (Moore *et al*., 2002). The atmospheric input of trace metals varies markedly spatially and termporally, and is of a similar magnitude as the riverine input. However, aeolian fluxes impact directly on the oceanic euphotic zone, while fluvial inputs are subjected to considerable modification in estuarine and coastal waters (Jickells, 1995).

Aluminum is a major component of continental materials and is present in seawater at low concentrations in regions devoid of large dust deposition due to the short residence time of aluminum in surface waters (3–5 yr; Orians and Bruland, 1986). Therefore, dissolved aluminum concentrations are an excellent tracer of atmospheric inputs to the ocean. A study by Vink and Measures (2001), using both a model of dust deposition (Measures and Brown, 1996) and dissolved aluminum concentrations in the Atlantic, has demonstrated that surface-water aluminum concentrations can be utilized to study the spatial and interannual variations of aeolian input. Concomitant with the aluminum concentrations, dissolved iron measurements were also carried out. At the interface between the canary current and the south equatorial current, a similar trend of maxima and minima in both the iron and aluminum concentrations was observed, implying a common atmospheric source. Although iron concentrations in the oceans are influenced by atmospheric inputs, low iron values in the surface waters of South Atlantic were observed, where aluminum concentrations suggested high dust deposition indicating that other factors such as, solubility and biological removal are more important in controlling iron distributions.

The maximum concentration of iron in oceanic surface seawater is controlled by the solubility of inorganic forms and the availability of organic complexing ligands to promote higher solubilities (Zhu *et al*., 1997; Jickells and Spokes, 2001; Vink and Measures, 2001). Perhaps the greatest uncertainty in estimating the impact of this atmospheric input on the oceans is the estimate of the percentage of trace metals associated with dust that is soluble upon entering the ocean. For iron, recent estimates are between 1% and 10%. Jickells and Spokes (2001) in a review suggest

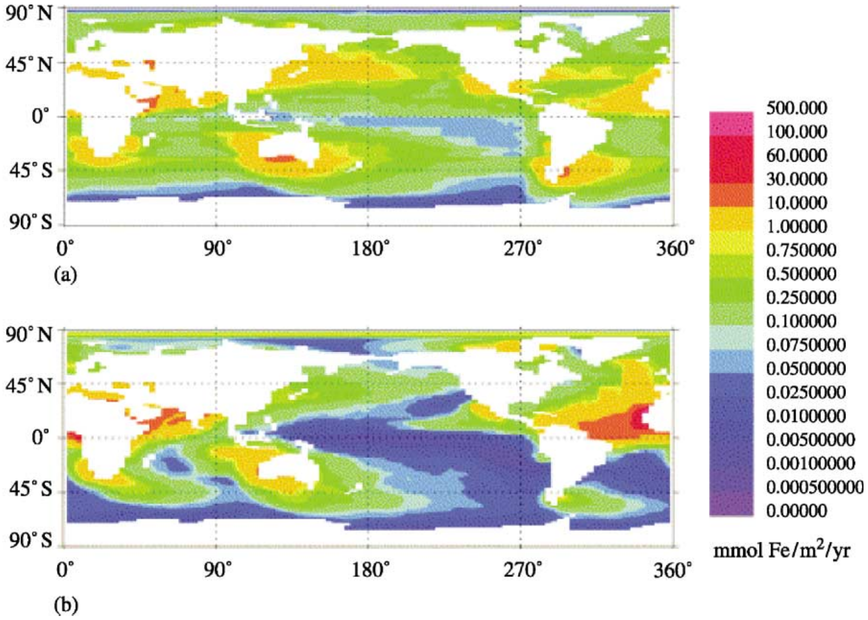

Figure 7 Modeled global estimates of aeolian iron deposition from: (a) Tegen and Fung (1994, 1995) and (b) Mahowald *et al*. (1999) (source Moore *et al*., 2002).

the mean solubility of iron from atmospheric dust is ~2%. New estimates indicate that ~40% of the world's oceans are limited by the trace metal iron. These regions are primarily located in remote regions where the supply of nutrients is high. In the remote subtropical gyres of the oceans, the source of nutrients and iron from vertical mixing or upwelling is small and, therefore, the atmospheric supply of iron is the dominant input. In the North Pacific, the input of Asian dust is at a maximum in the spring and this input may significantly increase the primary production during this time. The atmospheric input of iron to the central gyres can also be important with respect to nitrogen fixation, a process that requires iron as a metal co-factor (see Chapter 6.05). The variability in atmospheric input of trace metals such as iron can be extreme—the variability ranges from rapid day-to-day changes as a result of dust storms in Asia, to seasonal changes, to decadal changes (Jickells, 1995; Zhu *et al.*, 1997). Less is known about the mean solubility of other biologically important trace metals such as zinc and manganese.

An excellent example of the atmospheric input of a trace metal strongly influencing its surface-water concentration is lead. Tetraethyl lead, an anti-knock gasoline additive, was used extensively in the 1960s and 1970s, with its usage peaking in the late 1970s and then markedly declining in the 1980s and 1990s as a result of actions taken under the Clean Air Act of 1970 (Nriagu, 1989). This extensive use of leaded gasoline resulted in a large anthropogenic lead signal in atmospheric dust, particularly downwind of industrialized nations. Pioneering work of Patterson and co-workers (Schaule and Patterson, 1981, 1983; Flegal and Patterson, 1983) on the distribution of lead in the major central gyres of the Atlantic and Pacific oceans graphically point out how this anthropogenic atmospheric lead input markedly perturbed the distribution of lead in the different ocean basins at the peak of its input in the late 1970s and early 1980s (Figure 8). Due to the prevailing wind pattern, the North Atlantic received the brunt of the US lead input to the oceans and contained markedly elevated concentrations of lead in the upper 1,000 m. In contrast, the remote South Pacific central gyre had surface lead concentrations over an order-of-magnitude lower. Subsequent to this work, Boyle and co-workers (Wu and Boyle, 1997) presented results from a 16-year time series of lead concentrations in the western North Atlantic

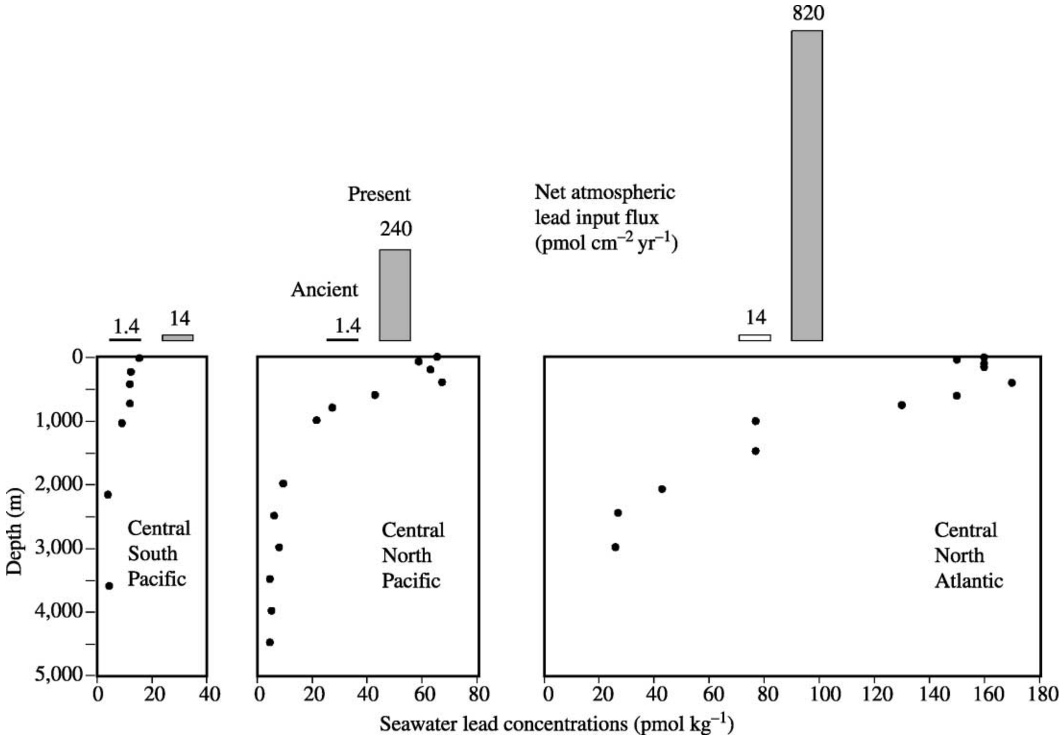

Figure 8 Vertical profiles of dissolved lead in the central North Atlantic (34° 15′ N, 66° 17′ W; data from Schaule and Patterson, 1983), the central North Pacific (32° 41′ N, 145° W; data from Schaule and Patterson, 1981), and the central South Pacific (20° S, 160° W; source Flegal and Patterson, 1983). Estimates of the atmospheric input at the time of sampling and in ancient times prior to the large anthropogenic lead input are also shown (Flegal and Patterson, 1983).

showing that lead concentrations decreased markedly during the decade of the 1980s and that this decrease can be attributed to the phasing out of leaded gasoline in the US.

6.02.2.3 Hydrothermal

It has been estimated, using arguments based upon the ^{3}He anomaly and heat flux, that the entire ocean mixes through hydrothermal vent systems, undergoing high-temperature interaction with fresh oceanic basalt every 8–10 Myr, leading to the production of high temperature (~350 °C), acidic (pH~3.5), reducing, sulfide- and metal-rich hydrothermal fluids (Edmond *et al.*, 1979; von Damm *et al.*, 1985). This ridge crest hydrothermal activity has proven to be the major oceanic sink for the major ions, magnesium, and sulfate, and to be a major source for trace metals such as iron and manganese (see Chapter 6.08). Iron and manganese concentrations in the 350 °C vent waters can be a million-fold higher than in the surrounding seawater. Much of the iron, however, is rapidly precipitated; initially either as iron sulfides and then oxidized to iron oxyhydroxide precipitates, or rapidly oxidized from the soluble Fe(II) form to insoluble Fe(III), and deposited as sediments over the mid-ocean ridges. The dissolved manganese can advect further away from the vent source prior to its microbially mediated oxidation and precipitation (Cowen *et al.*, 1998). The hydrothermal input of iron and manganese, however, is essentially all scavenged and removed in the deep sea prior to having a chance to mix back into the surface waters.

6.02.3 REMOVAL PROCESSES

6.02.3.1 Active Biological Uptake in the Surface Waters

6.02.3.1.1 Lessons from laboratory studies

A great deal of insight has been gained from well-defined laboratory studies of the effects of trace metals on phytoplankton growth rates, which in turn has provided knowledge on the control of trace metals in the upper water column by biological processes (see Chapter 6.05). Culture media have been designed in which the concentration and speciation of trace metals are controlled by the use of strong chelating ligands such as EDTA (Morel *et al.*, 1979; Price *et al.*, 1988/89; Sunda, 1988/89). The rate of uptake of a trace metal (M) is usually proportional to its free-metal concentration $[M^{2+}]$ or its unchelated concentration, $[M']$ (defined as the sum of the kinetically labile inorganic species of M). The $[M']$ and $[M^{n+}]$ are related by their inorganic side reaction coefficient ($\alpha = [M']/[M^{n+}]$). The EDTA chelated metal can act as a metal ion buffer that maintains $[M^{n+}]$ and $[M']$ at constant values in the media. By judiciously varying the EDTA and total metal concentrations, the experimental $[M^{2+}]$ and $[M']$ can be controlled over a wide range.

Diatoms are particularly important in biogeochemical cycles because of their role as major players in new and export production (Smetacek, 1999). Along with the assimilation and export of carbon, nitrogen, phosphorus, and silicon, diatoms also play an important role in the export of bioactive trace metals from surface waters. Sunda and Huntsman (1995a) have carried out extensive laboratory studies on iron uptake by coastal and oceanic diatoms. Figure 9 presents the cellular Fe/C (μmol mol^{-1}) ratio in diatoms as a function of the estimated $[Fe']$. These diatoms exhibit an increasing cellular Fe/C ratio as the $[Fe']$ in the media increases. At elevated $[Fe']$ in the media, the diatoms exhibit luxury uptake with the two coastal species reaching cellular Fe/C values that were 20–30 times higher than those estimated to be required for maximum growth (Sunda and Huntsman, 1995a). It has been suggested that this high uptake rate and storage capacity in the diatoms at elevated $[Fe']$ allows these species to accumulate excess iron during periods of high iron availability, that can then be passed on to their progeny and utilized when the dissolved iron may later be drawn down to concentrations limiting growth rates (Sunda and Huntsman, 1995a). This can be an effective strategy for diatom blooms in coastal upwelling regimes.

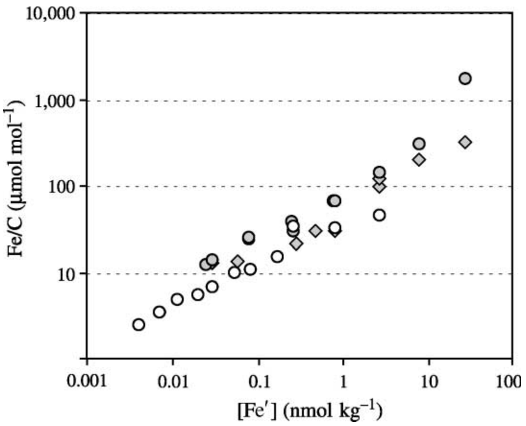

Figure 9 The relationship between the intracellular Fe/C ratio as a function of the inorganic iron concentration, $[Fe']$, for three diatoms species, *Thalassiosira oceanica* (○) an oceanic species (●), and two coastal species *Thalassiosira weissflogii*, and *Thalassiosira pseudonana* (◇) (source Sunda and Huntsman, 1995a).

6.02.3.1.2 Non-Redfieldian assimilation

Figure 9 is important with respect to removal of iron from the surface ocean. Nitrogen and phosphorus are assimilated and removed from the surface ocean at a ratio within about a factor of 2 of the Redfield ratio (Falkowski, 2000; Karl, 2002). Differences are observed at time-series stations in the North Pacific and North Atlantic (HOTS and BATS) that vary depending upon the source of nitrogen; however, they generally vary by less than a factor of 2. In contrast, there is no constant Redfield ratio of Fe/C; the Fe/C ratio in diatoms can vary by a factor of 100 depending upon the availability of iron and whether they are oceanic or coastal species. Interestingly, oceanic species have evolved to "get by" at lower iron concentrations than coastal species (Sunda and Huntsman, 1995a). Diatoms are also the type of phytoplankton most responsive to episodic changes in iron and nutrient inputs as demonstrated in each of the novel mesoscale iron-enrichment experiments (Martin *et al.*, 1994; Coale *et al.*, 1996; Boyd *et al.*, 2000). Their ability to maximize iron uptake and to store luxury uptake, can be a major factor in controlling iron concentrations in surface seawater. Bruland *et al.* (2001) examined this process in coastal diatoms under upwelling conditions and argued that iron is removed preferentially to nitrate in coastal upwelling regimes and tends to drive the system towards iron limitation. The amount of uptake of silicic acid by diatoms relative to the assimilation of nitrate and phosphate has been shown to depend on iron availability (Hutchins and Bruland, 1998; Takeda, 1998). Under iron-replete conditions, the silicon and nitrogen uptake is roughly equal, while under low-iron conditions diatoms exhibit Si/N uptake ratios of ~3. Under low iron concentrations the suppression of iron-containing enzymes such as nitrate or nitrite reductase has been confirmed for the chain-forming diatoms in the laboratory (de Baar *et al.*, 2000), resulting in reduced uptake of nitrogen relative to phosphorus and N/P ratios of 4–6 as compared to ~12–14 at adequate iron supply.

Studies have also been carried out on other essential trace metals such as zinc (Sunda and Huntsman, 1992, 1995b), and similar relationships between Zn/C and $[\mathrm{Zn}^{2+}]$ have been observed. In studies with the diatom *Thalassiosira oceanica*, the Zn/C (μmol mol^{-1}) ratio varied from 0.2 at $[\mathrm{Zn}^{2+}]$ of 10^{-13} M to ~40 at $[\mathrm{Zn}^{2+}]$ of 10^{-9} M (Figure 10). As with iron, there is more than 100-fold variation in the Zn/C ratio in diatoms as a function of $[\mathrm{Zn}^{2+}]$. The uptake of cadmium by diatoms is somewhat unique and is dependent not only upon the $[\mathrm{Cd}^{2+}]$, but also on $[\mathrm{Zn}^{2+}]$ (Sunda and Huntsman, 1998). At elevated $[\mathrm{Zn}^{2+}]$, cadmium assimilation and Cd/C ratios in diatoms are low. Under zinc depletion, however, the uptake of cadmium and Cd/C ratios markedly increase. Morel and co-workers (Price and Morel, 1990; Lee and Morel, 1995) have shown that cadmium can functionally replace zinc and that diatoms have a carbonic anhydrase enzyme utilizing cadmium instead of zinc as a metal co-factor. Thus, under low-zinc conditions, the assimilation of cadmium markedly increases and results in the depletion of cadmium in surface water. This is an example of where the cellular uptake of one metal, cadmium, responds to a complex matrix of other metals such as zinc. Cullen *et al.* (2003) provided evidence that the effect of iron limitation on resident diatoms in the Southern Ocean is to decrease growth rates, leading to elevated cellular cadmium content. In this case the assimilation of carbon, nitrogen, and phosphorus was markedly decreased as a result of iron limitation, but cadmium assimilation continued, leading to enhanced cellular Cd/P ratios.

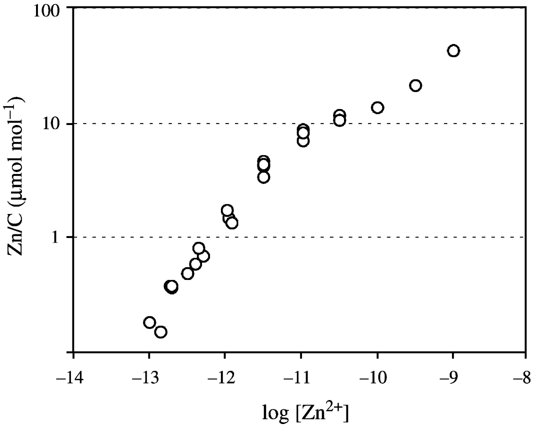

Figure 10 The relationship between the intracellular Zn/C ratio as a function of the free ionic zinc concentration, $[\mathrm{Zn}^{2+}]$, for an oceanic diatom species *Thalassiosira oceanica* (source Sunda and Huntsman, 1992).

For copper, the cellular metal/carbon ratios vary in more of a sigmoidal fashion, with what appears to be a region of varying $[\mathrm{Cu}^{2+}]$ with the Cu/C ratio somewhat constant and regulated (Sunda and Huntsman, 1995c). The Cu/C ratio in diatoms, however, still varies by roughly a factor of 100 over a wide range of concentrations of $[\mathrm{Cu}^{2+}]$ and has been implicated as an important factor in controlling the distribution of copper in the oceans (Sunda and Huntsman, 1995c).

Trace metals for which active biological assimilation may be an important factor in controlling surface-water concentrations and distributions include the first-row transition metals iron, zinc, manganese, copper, nickel, and cobalt, along with cadmium. Bruland *et al.* (1991) compiled data on the composition of plankton in the Pacific taken from two sources (Martin and Knauer, 1973; Martin *et al*., 1976) and excluded only data with an aluminum content >4 μmol g^{-1} (>100 μg g^{-1}) dry weight in an attempt to minimize the contribution from aluminosilicates minerals. Metal/carbon ratios for iron were close to 50 μmol mol^{-1}, Zn/C ranged from 8 μmol mol^{-1} to 17 μmol mol^{-1}, while Mn/C ratios averaged 3.6 μmol mol^{-1}. These M/C values for iron and zinc in diatom samples from the field off central California lie within the range expected for these region based upon laboratory studies. Biological assimilation of these metals at such M/C ratios with subsequent export of a fraction of this material to the deeper water column is particularly important in influencing the oceanic distributions of iron and zinc. These are two of the trace elements that exhibit marked surface depletion due to their involvement in this biological cycle.

6.02.3.2 Passive Scavenging

6.02.3.2.1 Adsorption/desorption processes

In addition to the role of active assimilation of required trace metals by phytoplankton, there is also passive scavenging of trace metals onto the wide variety of relatively high affinity surface sites on both living and dead particulate material existing in the surface waters. The combined process of surface adsorption, followed by particle settling, is termed scavenging (Goldberg, 1954; Turekian, 1977). Such binding is effectively "passive," in contrast with the active uptake of essential trace metals. Examples of trace metals implicated in such scavenging from surface waters include lead, aluminum, gallium, and the radioactive isotopes of thorium.

6.02.3.2.2 Lessons from radionuclides

Thorium, with its four different radioactive isotopes of greatly differing half-lives, is an excellent tracer which provides insight into the rates and the process of scavenging. Thorium isotopes and their half-lives are: ^{232}Th, $\tau_{1/2} = 1.4 \times 10^{10}$ yr (essentially ^{232}Th can be considered a stable isotope); ^{230}Th, $\tau_{1/2} = 7.54 \times 10^4$ yr with ^{234}U as a parent; ^{228}Th, $\tau_{1/2} = 1.91$ yr with ^{228}Ra as a parent; and ^{234}Th, $\tau_{1/2} = 24.1$ d with ^{238}U as a parent. Two conceptual models that have been used to model particle reactive thorium data are presented in Figure 11. Figure 11(a) incorporates reversible exchange and remineralization of the particles, while Figure 11(b) uses a net scavenging rate constant to examine the net scavenging of thorium. Figure 12 presents the distribution of the net scavenging rate constant of ^{234}Th in surface waters of the Pacific. The scavenging intensity of ^{234}Th varies dramatically between oligotrophic gyres of the North Pacific and South Pacific and productive regions such as the subarctic Pacific, the upwelling regime off central California and the equatorial Pacific. Values of the net scavenging rate constant in the surface mixed layer of the oligotrophic gyres were between 0.009 d^{-1} and 0.003 d^{-1} (yielding a mean life of dissolved ^{234}Th with respect to particle scavenging of 100–300 d). In contrast, in productive regions such as the subarctic Alaskan Gyre and intense coastal upwelling regimes off central California, the net scavenging rate constants were 0.11–0.10 d^{-1} (mean life of 9–10 d) and 0.175–0.125 d^{-1} (mean life of 6–8 d). The net scavenging rate constant has been argued to be proportional to new or export production (Coale and Bruland, 1987) and has been observed to be most intense in regimes of high particle production with substantial export of this material from the surface waters, and least intense in regions of lower primary production where regenerated production dominates.

Aluminum and gallium are two trace metals with hydrolysis chemistry similar to that of thorium and the affinity of a metal cation to form these hydrolysis species has been suggested as an important parameter in models for adsorption and scavenging processes. Orians and Bruland (1986, 1988) have presented data for aluminum and gallium (Figure 13) at some of the same stations where net thorium scavenging rates were determined (Figure 12). The surface-water concentrations of aluminum and gallium should be a function of the magnitude of sources relative to their scavenging removal rate. Both of these metals exhibit higher concentrations in the surface waters of the oligotrophic central gyres, with much lower values observed towards the north and eastern boundaries where rates of export production and ^{234}Th scavenging are higher. Undoubtedly, since Fe(III) is another trace metal with similar hydrolysis chemistry, such scavenging would also take place for it. It is, however, difficult to separate such passive scavenging from active assimilation that also occurs with iron.

Thorium isotopes have also been used to gain insight into scavenging in deep waters. Using a combination of thorium isotopes, investigators have been able to determine the dynamics of thorium scavenging (Bacon and Anderson, 1982; Nozaki *et al*., 1987; Clegg *et al*., 1991; Murname, 1994; Roy-Barman *et al*., 1996). These studies have provided evidence for a dynamic system whereby thorium isotopes appear to be reversibly scavenged from the deep sea onto fine particles, these particles are packaged into larger particles that sink and then either disaggregate or are

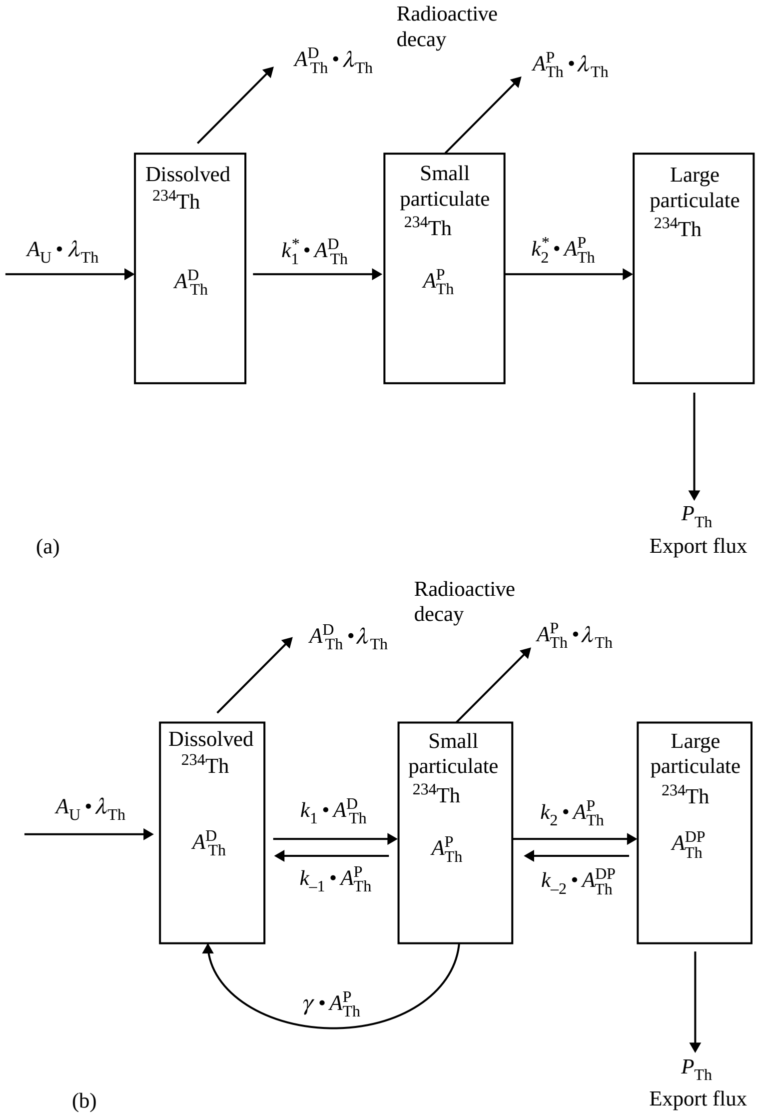

Figure 11 Conceptual models of thorium scavenging (Coale and Bruland, 1985; Bruland and Coale, 1986; Clegg *et al.*, 1991). (a) The surface water ^{234}Th net scavenging model. This model incorporates two different size classes of particles, small suspended particles and large sinking particles with the various sources and sinks for the activity (A) of ^{234}Th depicted. λ_{Th} is the decay constant of ^{234}Th, k_1^* is the net rate transfer of ^{234}Th from dissolved to suspended particles and k_2^* is the net rate of transfer of ^{234}Th from small suspended particles to large sinking particles. (b) A reversible scavenging model including desorption, particle disaggregation and remineralization for the deep sea. ^{230}Th and ^{234}Th can be both modeled to yield estimates of rate constants. Rate constants: k_1, adsorption onto small suspended particles and k_{-1}, desorption from small suspended particles; k_2, aggregation or packaging rate of small suspended particles into large sinking particles and k_{-2} is the disaggregation of large sinking particles and γ remineralization of carrier phases including respiration of organic matter or dissolution.

remineralized, and the thorium is either desorbed or released back into solution. In this manner, an individual thorium isotope might spend a total of 20–50 yr in the deep sea before burial in the sediments (see Chapter 6.09) and during this time undergo numerous reversible adsorption/desorption exchanges with particles that are continually aggregating into larger particles, sinking and disaggregating or being remineralized. Estimates of residence times of thorium in various forms within the deep sea suggest that an isotope might spend close to a year in the dissolved form prior to adsorption onto the surface of a small particle where it may reside for another four months prior to aggregating to a larger, more rapidly sinking particle. It might spend a few days sinking a few hundred meters prior to disaggregation and then a few months residing on the small particle prior to desorption or remineralization back into the dissolved phase

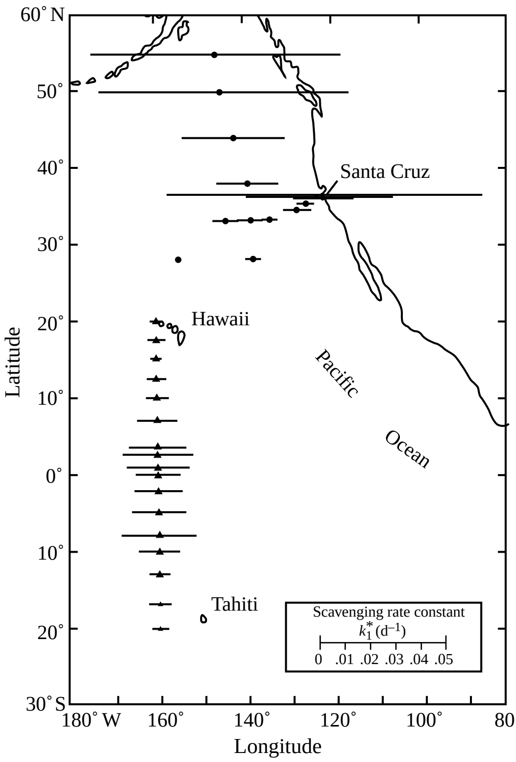

Figure 12 The net scavenging rate constant, k_1^* (d^{-1}), of ^{234}Th from the surface mixed layer of the Pacific Ocean (sources Bruland and Coale, 1986; Bruland and Beals, unpublished).

(Murname, 1994). Similar dynamic reversible exchange processes in the deep sea may be occurring for other trace metals such as iron, aluminum, gallium, and titanium.

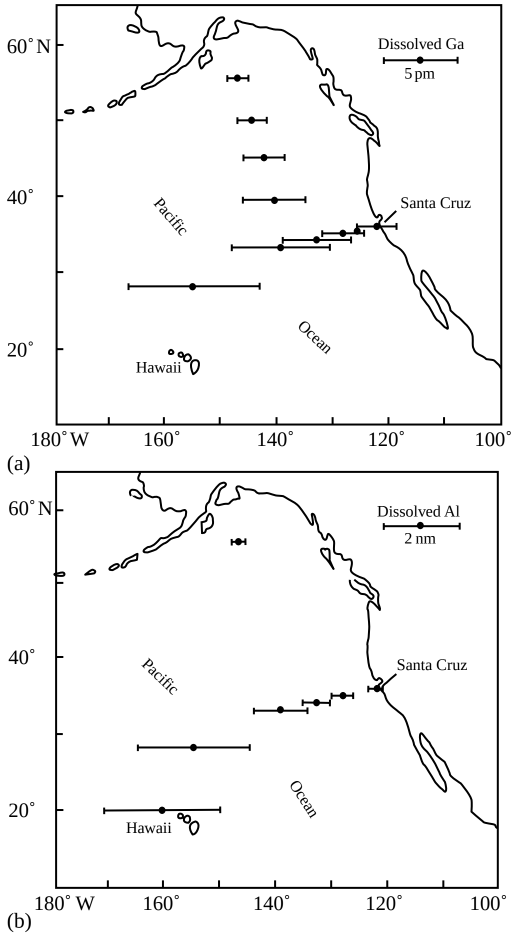

Figure 13 Concentrations of (a) dissolved gallium (data from Orians and Bruland, 1988) and (b) dissolved aluminum (data from Orians and Bruland, 1986) in the surface waters of the eastern North Pacific at stations for which ^{234}Th net scavenging rate data exist (see Figure 12).

6.02.4 INTERNAL RECYCLING

6.02.4.1 Recycling within the Water Column

Internal recycling is particularly relevant for nutrient-type trace metals that, like the macronutrients nitrate, phosphate, and silicic acid, undergo multiple cycles of assimilation into biogenic particulate material within surface waters and release or remineralization at depth. In this manner an element can undergo many internal cycles within the ocean prior to ultimate burial in sediments. For example, imagine an individual zinc ion delivered to the surface waters by upwelling or vertical mixing. It can be assimilated into a phytoplankton cell, where it might reside a day or two prior to being grazed. In the open ocean the bulk of this phytoplankton zinc and other nutrients will be remineralized in the surface waters and available to undergo perhaps 5 or 10 such assimilation/remineralization cycles within the surface layer (Hutchins *et al.*, 1993; Hutchins and Bruland, 1994, 1995) prior to removal as an export flux in the form of a fecal pellet excreted from a zooplankter or a larger aggregate of particles. This particulate zinc can be remineralized in the deep sea as the fecal pellet serves as a source of food and nutrition for heterotrophic organisms in the deep sea. Remineralization of particulate zinc can occur at depth by the degradation of organic matter or the dissolution of the inorganic carrier phases (metal oxides, opal, calcite). Then perhaps a few hundred to a thousand years later this same zinc ion can be mixed back up into the surface waters. Numerous such cycles can occur during its $(10-50) \times 10^4$ yr odyssey in the oceans. Once finally removed via burial in the sediments, the zinc atom may have to wait ~100 Myr to be tectonically uplifted onto a continent and then another 100 Myr before it is exposed to continental weathering and makes its way via rivers or dust input back to the ocean.

6.02.4.2 Benthic Inputs

Upon settling to the surface sediments, trace metals can be recycled back into the dissolved phase and act as a source to the deep ocean. Pore-water concentrations of trace metals can be significantly higher than that observed in the overlying water column. Elevated pore-water concentrations suggested a potential for benthic fluxes of dissolved metals out of the sediment, which has been verified by direct measurements (Elderfield *et al.*, 1981; Westerlund *et al.*, 1986).

Trace metals in marine sediments are frequently associated with iron and manganese hydroxides and changes in the sediment redox chemistry near the sediment water interface can lead to alternating periods of reductive dissolution and oxidation of these phases. Depth profiles in the shelf waters off the coast of the Falkland Islands and SW Africa indicate a significant supply of dissolved iron (2–38 nmol kg^{-1}) to the overlying water column through reductive benthic processes (Bowie *et al.*, 2002). Iron concentrations just above the sediment interface were 12-fold higher than those observed at the surface. Benthic inputs of iron, cobalt, and manganese have been observed in the highly productive coastal waters of the North Sea (Tappin *et al.*, 1995). Trace-metal recycling through benthic inputs has the potential to supply trace metals back into surface waters. The dominant source of iron to waters off the coast of California is through sediment resuspension followed by upwelling (Johnson *et al.*, 1999; Bruland *et al.*, 2001).

6.02.5 COMPLEXATION WITH ORGANIC LIGANDS

Studies using electrochemical techniques have demonstrated that in surface seawater a major fraction of many trace metals, particularly the bioactive trace metals such as iron, zinc, copper, cobalt, and cadmium, are present as chelates with strong metal-binding organic ligands. These electrochemical methods employ sensitive stripping voltammetric analysis. Anodic stripping voltammetry (ASV), using a thin mercury film (TMF), rotating glassy carbon disk electrode (RGCDE) in the differential pulse (DP) mode, has been used in open ocean studies of copper (Coale and Bruland, 1988, 1990), zinc (Bruland, 1989), cadmium (Bruland, 1992), and lead (Capodaglio *et al.*, 1990). This method directly measures the kinetically labile [M$'$] (inorganic complexes and free metal), while the metal chelated with strong organic ligands is kinetically inert with respect to being detected by this method. ASV involves a deposition or concentration step that can be ~10 min or 20 min in duration where M$'$ is continually reduced and concentrated into the mercury amalgam. The DP stripping step involves ramping the potential in a positive direction and the measurement of the anodic stripping current as the metals are oxidized back into solution. Titrations of a sample with the metal of interest and determining [M$'$] at each titration point allow both the concentrations of the M-binding ligands and binding strengths (conditional stability constants) of the metal–ligand complexes to be determined. The number of trace metals that can be determined by ASV, however, is limited to those that can be reduced (and reoxidized) at appropriate potentials and that are soluble in a mercury amalgam.

A second powerful voltammetric approach that is amenable to a far broader group of trace metals is adsorptive cathodic stripping voltammetry (AdCSV). The application of AdCSV to speciation studies involves the addition of a well-characterized added ligand (AL) that sets up a competitive equilibrium with the natural ligands for the metal of interest (van den Berg, 1988). Most methods involve formation of a neutral biscomplex with the AL, $M(AL)_2^0$ (Bruland *et al.*, 2000). The ALs generally form planer biscomplexes with the metal of interest that have a strong tendency to adsorb on the surface of a hanging mercury drop electrode, whereas the natural metal–ligand complexes do not. After an appropriate adsorption or accumulation time period, the potential is ramped in a negative direction (in either linear, DP or Osteryoung square wave (SW) mode) and the cathodic stripping current is measured as the metal (and sometimes also the AL) is reduced at the electrode surface. The use of these AdCSV methods does not require the metal to be soluble in a mercury amalgam and thus can be used for a wide variety of trace metals. Metal titrations and the determination of the $M(AL)_2^0$ concentration at each titration point allows the determination of natural, strong metal-binding ligand concentrations and their conditional stability constants. The use of AdCSV methods has been applied to studies of the speciation of iron (van den Berg, 1995; Rue and Bruland, 1995; Bruland and Rue, 2001), copper (van den Berg, 1984; Moffett *et al.*, 1990; Donat and van den Berg, 1992), zinc (van den Berg, 1985; Donat and Bruland, 1990; Ellwood and van den Berg, 2000; Lohan *et al.*, 2002), and cobalt (Saito and Moffett, 2001; Ellwood and van den Berg, 2001). It should be noted that "detection windows" of voltammetric techniques examine stability constants of metal-binding ligands specified by the technique, and that natural metal-binding organic ligands are not a single entity but rather classes of ligands with average values assigned.

Results of such voltammetric studies have demonstrated that complexation of trace metals with relatively specific and strong metal-binding organic ligands is important in oceanic surface waters. Greater than 99% of Fe(III) in surface waters is complexed with strong Fe(III)-binding organic ligands existing at sub-nanomolar concentrations in slight excess of the dissolved iron (Rue and Bruland, 1995; van den Berg, 1995; Wu and Luther, 1995; Powell and Donat, 2001; Boye *et al.*, 2003). Greater than 99% of copper exists as organic complexes (Coale and Bruland, 1988; Moffett, 1990). Approximately 98% of dissolved zinc in surface waters is complexed with organic ligands (Bruland, 1989; Donat and Bruland, 1990; Ellwood and van den Berg, 2000; Lohan *et al.*, 2002). Greater than 90% of cobalt exists complexed to strong cobalt-binding organic ligands (Saito and Moffett, 2001; Ellwood and van den Berg, 2001) and ~80% of cadmium in surface waters is complexed with organic ligands (Bruland, 1992).

We know little about the chemical structure or architecture of the organic ligands involved in binding metals in seawater. There have been recent advances, however, into the structure and function of marine siderophores. The conditional stability constants of the marine siderophores so far examined are similar to the stability constants of the natural Fe(III)-binding ligands found in seawater (Barbeau *et al.*, 2001, 2003) and siderophores appear to constitute a significant fraction of the natural Fe(III)-binding organic ligands in seawater (Macrellis *et al.*, 2001). Siderophores are defined as low molecular weight organic chelators with a very high and specific affinity for Fe(III), the biosynthesis of which is regulated by iron levels, and whose function is to mediate iron uptake by microbial cells.

The selectivity of siderophores for Fe(III) is achieved through optimal selection of metal-binding groups, the number of binding units, and their stereochemical arrangement (Boukhalfa and Crumbliss, 2002). Most siderophores are hexadentate and incorporate hydroxamate, catecholate, and/or α-hydroxy carboxylate binding subunits arranged in different architectures. Barbeau *et al.* (2003) have presented a summary of many of the marine siderophores groups produced by both heterotrophic and photosynthetic marine bacteria and characterized the photochemical reactivity of the different Fe(III)-binding functional groups. Hydroxamate groups are photochemically resistant regardless of Fe(III) complexation. Catecholates are susceptible to photo-oxidation in the uncomplexed form, but stabilized against photo-oxidation when ferrated. α-Hydroxy carboxylate groups are stable as the uncomplexed acid, but when coordinated to Fe(III) these moieties undergo light-induced ligand oxidation and reduction of Fe(III) to Fe(II). These photochemical properties appear to determine the reactivity and fate of Fe(III)-binding siderophores in ocean surface waters (Barbeau *et al.*, 2003).

Other possible candidates of natural Fe(III)-binding ligands in seawater are porphyrin-type ligands released as degradation products of cytochrome-containing systems (Rue and Bruland, 1997). As yet, little is known about this possibility. In addition, little is known about the structure, functional groups, or architecture of other metal-binding organic ligands in seawater. What is known is that there appear to be small concentrations of strong and relatively specific metal-binding organic ligands that play an important role in the chemical speciation of quite a few of the bioactive trace metals in the sea.

6.02.5.1 Copper

Copper provides an interesting example of a trace metal that is an essential, required element, but that can be toxic at relatively low concentrations. It can be considered the "Goldilocks" metal. Surface-water concentrations in the open ocean are ~1 nmol kg^{-1}. Without organic complexation, the free copper concentration would be approximately a factor of 20 lower than the total dissolved concentration, with $Cu(CO_3)^0$ predicted to be the dominant species. This would yield $[Cu^{2+}]$ concentrations $\sim 0.5 \times 10^{-10}$ M or $10^{-10.3}$ M. This concentration would be toxic to many oceanic phytoplankton, particularly the prokaryotic photosynthetic bacteria such as synechococcus (Brand *et al.*, 1986). Figure 14(b) presents the actual vertical distribution of $[Cu^{2+}]$ in the upper 500 m of the Northeast Pacific. Coale and Bruland (1988, 1990) observed a slight excess of a strong copper-binding class of organic ligands, called L_1. This class of strong copper-binding ligands was found to occur in surface waters at concentrations of 1–2 nmol kg^{-1} and its presence led to greater than 99.8% of the copper being chelated to this class of ligands. As a result, $[Cu^{2+}]$ was reduced by close to a factor of 1,000 and exists at concentrations $\sim 10^{-13}$ M, which is a concentration not toxic to phytoplankton. Moffett and Brand (1996) have shown that cyanobacteria when stressed with slightly elevated $[Cu^{2+}]$ can produce a ligand with a similar conditional stability constant. It appears that, somehow, the phytoplankton of the open ocean, particularly the prokaryotic phytoplankton, are controlling the external concentration of free copper by producing a strong copper-binding ligand that reduces the $[Cu^{2+}]$ to levels that are no longer toxic. As a result, the $[Cu^{2+}]$ in surface waters is buffered by the L_1 class of ligands at a concentration that is "not too little" and "not too much," but "just right"; thus, the "Goldilocks example." This buffering of $[Cu^{2+}]$ also influences its distribution

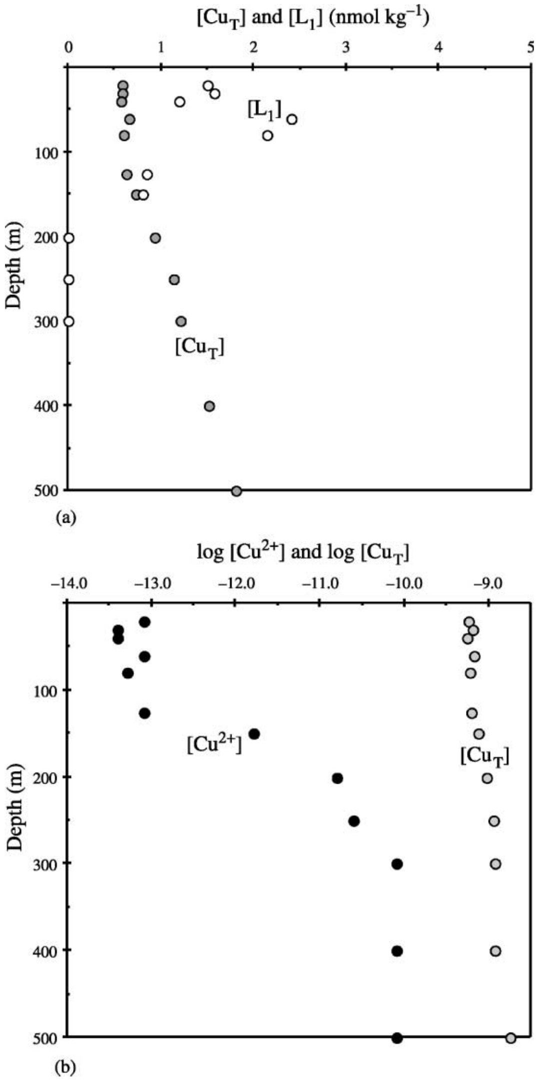

Figure 14 Concentration profiles of (a) total dissolved copper, $[Cu_T]$, and strong copper-binding organic ligands, $[L_1]$, and (b) free $[Cu^{2+}]$ and $[Cu_T]$ in the upper 500 m of the North Pacific (source Coale and Bruland, 1988).

and, because this chelated form is unavailable biologically, the dissolved copper is not depleted to a great degree in oceanic surface waters.

6.02.5.2 Iron

Dissolved iron provides an example of a bioactive, essential trace metal that is depleted in oceanic surface waters to such an extent that it has been estimated to be the limiting nutrient in ~40% of the world's oceans (Moore *et al*., 2002). In particular, iron has been shown to be the limiting nutrient in the HNLC regions of the Southern Ocean, the equatorial Pacific, and the subarctic Pacific (Martin *et al*., 1994). Not only does iron exist at extremely low concentrations in surface waters, its chemical speciation is dominated by complexation with Fe(III)-binding organic ligands. The initial evidence that dissolved iron is strongly chelated by natural Fe(III)-binding organic ligands in seawater was provided by van den Berg (1995), Rue and Bruland (1995), and Wu and Luther (1995). Results from surface waters of the equatorial and North Pacific oceans (Rue and Bruland, 1995, 1997) indicate that two classes of Fe(III)-binding ligands exist. There appears to be 0.3–0.4 nmol kg^{-1} of particularly strong ligands (an L_1 class) with a conditional stability constant (with respect to Fe(III)$'$) of $10^{12.5}$–10^{13} M^{-1}. In addition, there is a more variable class of weaker ligands (an L_2 class) existing at concentrations of 0.2–1.5 nmol kg^{-1} with a conditional stability constant of $10^{11.5}$–$10^{11.8}$ M^{-1}. This is a case where it appears that microorganisms are essentially carrying out "chemical warfare" in their attempts to acquire this metal.

Marine siderophores produced by both heterotrophic and photosynthetic bacteria that have been so far examined have conditional stability constants consistent with the classes of natural organic ligands observed in seawater (Barbeau *et al*., 2001, 2003). For marine siderophores to be competitive for binding Fe(III) in surface seawater, they would have to be this strong. Barbeau *et al*. (2001) have also shown that photodegradation products of the original siderophores have weaker conditional stability constants similar to the L_2 class of ligands observed by Rue and Bruland (1995, 1997). It is known that many microorganisms are able to not only utilize their own siderophores, but in addition, can assimilate numerous other bacteria's siderophores (Wilhelm and Trick, 1994). Eukaryotic diatoms are thought to not have the receptor sites to assimilate Fe(III)–siderophores directly. There is evidence, however, that diatoms can utilize cell-surface reductase systems to reduce the Fe(III) bound to the siderophore, and Fe(II) can dissociate and become available either as Fe(II) or can be reoxidized to Fe(III) and become available for assimilation (Maldonado and Price, 1999). Barbeau *et al*. (2001) have shown that iron associated with the more weakly held photoproduct of marine siderophores is more readily available than the original Fe(III)–siderophore. Hutchins *et al*. (1999) have also addressed the issue of the availability of Fe(III) bound to various siderophores and other ligands and have observed differences in availability. Fe(III)–porphyrin complexes seem to be more readily available to the eukaryotic diatoms, while Fe(III)–siderophores are more readily available by the prokaryotic phytoplankton community.

In the iron-limited regions of the ocean, iron is cycled through the planktonic community so rapidly that an individual iron atom may be in a different form each day. It may exist dissolved as an Fe(III)–siderophore one day, be part of the intracellular photosynthetic machinery of a photosynthetic bacteria the next day, be regenerated as an iron–porphyrin cell lysis product the next day, and then rapidly reassimilated by a diatom. In this case, the iron that is biologically available is changing on a day-to-day basis. Of interest to this chapter is the eventual export of iron from the surface water as the diatom is grazed by a copepod and a part of the undigested residue of the diatom and its associated iron is removed from the surface layer as a fecal pellet to be transported into the deep sea where it can be remineralized and either scavenged or eventually mixed back into the surface layer once again. Interestingly, it has been argued that Fe(III)-binding organic ligands observed in the deep sea (Rue and Bruland, 1995) play an important role in allowing the dissolved iron in the deep sea to exist at concentrations on the order of a nmol kg^{-1} (Johnson *et al*., 1997). This is a higher concentration than would be expected from estimates of inorganic solubility (Liu and Millero, 2002).

6.02.5.3 Zinc

Field studies have revealed that there are nanomolar concentrations of strong zinc-binding organic ligands in surface waters (Bruland, 1989; Donat and Bruland, 1990; Ellwood and van den Berg, 2000; Lohan *et al*., 2002) that play an important role in chelating zinc in surface waters. Figures 15(a) and (b) presents data from the North Pacific (Bruland, 1989) and it is apparent that ~98% of the dissolved zinc in surface waters exists in a chelated form with organic ligands. Although we have insight into the concentrations and conditional stability constants of these ligands, we know little or nothing about their functional character or molecular architecture. There are no immediate solubility constraints on the zinc concentration and it does not undergo redox cycling so that the benefits conferred by complexation upon iron availability do not apply to zinc. Unlike copper, zinc is not toxic to phytoplankton at concentrations observed in the open ocean. There appears to be no immediate advantage to the phytoplankton community in reducing [Zn^{2+}] through organic complexation.

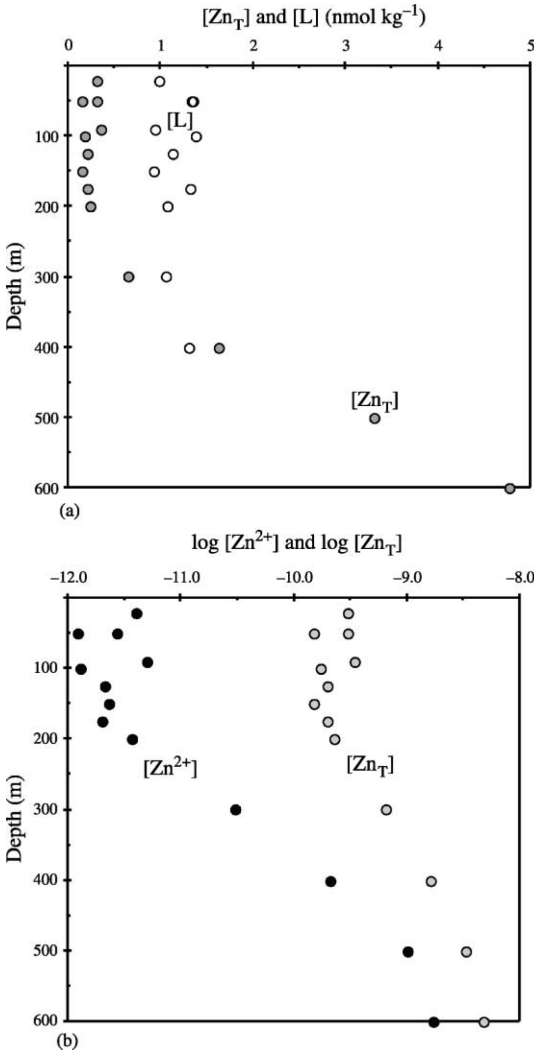

Figure 15 Concentration profiles of (a) total dissolved zinc, [Zn$_T$], and strong zinc-binding organic ligands, [L] and (b) free [Zn^{2+}] and [Zn$_T$] in the upper 600 m of the North Pacific (source Bruland, 1989).

One interesting idea is that this might be an example of "smart banking" by the plankton community. By having the bulk of the zinc chelated and presumably less bioavailable, the removal rate of zinc by the biota will be less (see Figure 10). As discussed previously in Section 6.02.3.2.1, the Zn/C ratio in diatoms is dependent upon the [Zn^{2+}]. Therefore, by markedly decreasing [Zn^{2+}] with the production of a zinc-binding organic ligand, the removal rate of zinc will be decreased and its residence time in the surface water increased, e.g., the capital is preserved. Conversely, some of the zinc-binding ligands may be a zinc siderophore-type compound whereby certain microorganisms are attempting to gain an advantage for this potentially biolimiting element.

Voltammetric techniques have provided a powerful tool for measuring the speciation of trace metals at low concentrations. Most of the bioactive trace metals have now been analyzed using these techniques. Knowledge of the inorganic, organic, and free metal forms in the dissolved phase is critical as the different forms are involved in very different biological and geochemical interactions and hence the cycling of trace metals within the ocean. Studies of trace-metal speciation have influenced ideas about the role of trace metals in biological systems. The previous conceptions that trace metals bound to these ligands were not bioavailable has undergone a complete change since the discovery that iron bound to siderophores can be readily accessed by phytoplankton. It may be that the strong cobalt-binding ligands observed by Saito and Moffett (2001) and Ellwood and van den Berg (2001) are a type of "cobalophore" and play a role similar to siderophores with iron. The production of highly specific metal-binding ligands by phytoplankton has led to many interesting questions which are yet to be resolved.

New analytical techniques are emerging such as electrospray ionization mass spectroscopy (ESI-MS) that may prove useful in gaining insight into the structure and functional groups of metal-binding organic ligands in seawater. First, however, the low concentrations of metal-binding ligands must be concentrated from the seawater matrix and isolated or separated from the rest of the dissolved organic matter. This will hopefully allow a better mechanistic understanding of the production and regulation of these ligands in the upper water column and hence increase the understanding of the cycling of dissolved trace metals in the oceans.

In summary, we have presented a general overview of the major controls of trace metals in seawater developed from the extensive research on trace metals over the last few decades. We wanted the reader to gain a first order understanding and not present a comprehensive review on the distribution of each trace metal. Each of the trace metals discussed will undoubtedly prove to have unique characteristics and subtle differences from this simplified version, yet the comparison with these simplified characteristics will serve as a good spring board to a more complete understanding. We have gained an insight into many of the processes affecting trace-metal cycling within the oceans, which has revealed many interesting questions still to be answered. Developments in isolating and characterizing metal-binding organic ligands should elucidate further the controls of trace metals in the upper water column. While in the mesopelagic zone the characterization of trace-metal fluxes and the processes involved in remineralization will greatly enhance our understanding of trace-metal cycling both within this region and exchanges between the benthos and the upper photic zone.

REFERENCES

Anbar A. D., Wasserburg G. J., Papanastassiou D. A., and Anderson P. S. (1996) Iridium in natural waters. *Science* **273**, 1524–1528.

Bacon M. P. and Anderson R. F. (1982) Distribution of thorium isotopes between dissolved and particulate forms in the deep-sea. *J. Geophys. Res.* **87**, 2045–2050.

Barbeau K., Rue E. L., Bruland K. W., and Butler A. (2001) Photochemical cycling of iron in the surface ocean mediated by microbial iron(III)-binding ligands. *Nature* **413**, 409–413.

Barbeau K., Rue E. L., Trick C. G., Bruland K. W., and Butler A. (2003) The photochemical reactivity of siderophores produced by marine heterotrophic bacteria and cyanobacteria, based on characteristic iron(III)-binding groups. *Limnol. Oceanogr.* **48**, 1069–1078.

Boukhalfa H. and Crumbliss A. L. (2002) Chemical aspects of siderophore mediated iron transport. *Biometals* **15**, 325–339.

Bowie A., Maldonado M., Frew R. D., Croot P. L., Achterberg E. P., Mantoura R. F. C., Worsfold P. J., Law C. S., and Boyd P. W. (2001) The fate of added iron during a mesoscale fertilisation experiment in the Southern Ocean. *Deep-Sea Res. II* **48**, 2703–2743.

Boyd P. W., Watson A. J., Law C. S., Abraham E. R., Trull T., Murdoch R., Bakker D. G. E., Bowie A., Buesseler K. O., Chan H., Charette M. A., Croot P. L., Downing K., Frew R., Gall M. P., Hadfield M., Hall J., Harvey M., Jameson J., LaRoche J., Liddicoat M., Ling R., Maldonado M. T., McKay R. M., Nodder S., Pickmere S., Pridmore R., Rintoul S., Safi K., Sutton P., Strzepek R., Tanneberger K., Turner S., Waite A., and Zeldis J. (2000) A mesoscale phytoplankton bloom in the Polar Southern Ocean stimulated by iron fertilization. *Nature* **407**, 695–702.

Boye M. B., Aldrich A. P., van den Berg C. M. G., deJong J. T. M., Veldhuis M. J. W., and de Baar H. J. W. (2003) Horizontal gradient of the chemical speciation of iron in surface waters of NE Atlantic Ocean. *Mar. Chem.* **50**, 129–143.

Boyle E. A. (1988) Cadmium: chemical tracer of deep water oceanography. *Paleoceanography* **3**, 471–489.

Boyle E. A., Sclater F. R., and Edmond J. M. (1976) On the marine geochemistry of cadmium. *Nature* **263**, 42–44.

Boyle E. A., Edmond J. M., and Sholkovitz E. R. (1978) The mechanism of iron removal in estuaries. *Geochim. Cosmochim. Acta* **41**, 1313.

Brand L. E., Sunda W. G., and Guillard R. R. L. (1986) Reduction in marine phytoplankton reproduction rates by copper and cadmium. *J. Exp. Mar. Biol. Ecol.* **96**, 225–250.

Brewer P. G., Spenser D. W., and Robertson D. E. (1972) Trace element profiles from the GEOSECS II test station in the Sargasso Sea. *Earth Planet. Sci. Lett.* **16**, 111–116.

Broecker W. S. and Peng T. H. (1982) Tracers in the Sea. Eldigo Press, Palisades, NY.

Bruland K. W. (1980) Oceanographic distributions of Cd, Zn, Cu, and Ni in the North Pacific. *Earth Planet. Sci. Lett.* **47**, 176–198.

Bruland K. W. (1983) Trace elements in sea water. In *Chemical Oceanography* (eds. J. P. Riley and R. Chester). Academic Press, London, vol. 8, pp. 157–220.

Bruland K. W. (1989) Complexation of zinc by natural organic ligands in the central North Pacific. *Limnol. Oceanogr.* **34**, 269–285.

Bruland K. W. (1992) Complexation of cadmium by natural organic ligands in the central North Pacific. *Limnol. Oceanogr.* **37**, 1008–1017.

Bruland K. W. and Coale K. H. (1986) Surface water ^{234}Th/^{238}U disequilibria: spatial and temporal variations of scavenging rates within the Pacific Ocean. In *Dynamic Processes in the Chemistry of the Upper Ocean*, NATO Conference Series IV: Marine Sciences (eds. J. D. Burton, P. G. Brewer, and R. Chesselet). Plenum, New York, pp. 159–172.

Bruland K. W. and Franks R. P. (1983) Mn, Ni, Cu, Zn, and Cd in the western North Atlantic. In *Trace Metals in Seawater* (eds. C. S. Wong, E. A. Boyle, K. W. Bruland, J. D. Burton, and E. D. Goldberg). Plenum, New York, pp. 395–414.

Bruland K. W. and Rue E. L. (2001) Analytical methods for determination of concentrations and speciation of iron. In *The Biogeochemistry of Iron in Seawater* (eds. D. R. Turner and K. A. Hunter). Wiley, Chichester, pp. 255–289.

Bruland K. W., Knauer G., and Martin J. (1978a) Cadmium in Northeast Pacific waters. *Limnol. Oceanogr.* **23**, 618–625.

Bruland K. W., Knauer G., and Martin J. (1978b) Zinc in Northeast Pacific waters. *Nature* **271**, 741–743.

Bruland K. W., Donat J. R., and Hutchins D. T. (1991) Interactive influences of bioactive trace metals on biological production in oceanic waters. *Limnol. Oceanogr.* **36**, 1555–1577.

Bruland K. W., Orians K. J., and Cowen J. P. (1994) Reactive trace metals in the stratified central North Pacific. *Geochim. Cosmochim. Acta* **58**, 3171–3182.

Bruland K. W., Rue E. L., Donat J. R., Skabal S., and Moffett J. W. (2000) An intercomparison of voltammetric approaches to determine the chemical speciation of dissolved copper in a coastal seawater sample. *Anal. Chim. A* **405**, 99–113.

Bruland K. W., Rue E. L., and Smith G. J. (2001) The influence of iron and macronutrients in coastal upwelling regimes off central California: implications for extensive blooms of large diatoms. *Limnol. Oceanogr.* **46**, 1661–1674.

Burton J. D. and Statham P. J. (1990) Trace metals in seawater. In *Heavy Metals in the Marine Environment* (eds. P. S. Rainbow and R. W. Furness). CRC Press, Boca Raton, FL.

Byrne R. H., Kump L. R., and Cantrell K. J. (1988) The influence of temperature and pH on trace metal speciation in seawater. *Mar. Chem.* **25**, 163–181.

Capodaglio G., Coale K. H., and Bruland K. W. (1990) Lead speciation in surface waters of the eastern North Pacific. *Mar. Chem.* **29**, 221–238.

Chan L. H., Edmond J. M., Stallard R. G., Broecker W. S., Chung Y., Weiss R. F., and Ku T. L. (1976) Radium and barium at GEOSECS stations in the Atlantic and Pacific. *Earth Planet. Sci. Lett.* **32**, 258–267.

Chan L. H., Drummond D., Edmond J. M., and Grant B. (1977) On the barium data from the Atlantic GEOSECS expedition. *Deep-Sea Res.* **24**, 613–649.

Clegg S. L., Bacon M. P., and Whitfield M. (1991) Application of a generalized scavenging model to thorium isotope and particle data at equatorial and high latitude sites in the Pacific Ocean. *J. Geophys. Res.* **96**, 20665–20670.

Coale K. H. and Bruland K. W. (1985) ^{234}Th/^{238}U disequilibria within the California Current. *Limnol. Oceanogr.* **30**, 22–33.

Coale K. H. and Bruland K. W. (1987) Oceanic stratified euphotic zone as elucidated by ^{234}Th/^{238}U disequilibria. *Limnol. Oceanogr.* **32**, 189–200.

Coale K. H. and Bruland K. W. (1988) Copper complexation in the northeast Pacific. *Limnol. Oceanogr.* **33**, 1084–1101.

Coale K. H. and Bruland K. W. (1990) Spatial and temporal variability in copper complexation in the North Pacific. *Deep-Sea Res.* **37**, 317–336.

Coale K. H., Johnson K. S., Fitzwater S. E., Gordon R. M., Tanner S., Chavez F. P., Ferioli L., Sakamoto C., Rogers P., Millero F., Steinberg P., Nightingale P., Cooper D., Cochlan W. P., Landry M. R., Constantinou J., Rollwagen G., Trasvina A., and Kudela R. (1996) A massive phytoplankton bloom induced by a ecosystem-scale iron fertilisation experiment in the equatorial Pacific Ocean. *Nature* **383**, 495–501.

Cowen J. P., Betram M. A., Baker G. T., Feely R. A., Massoth G. J., and Summit M. (1998) Geomicrobial transformations of manganese in Gorda Ridge event plumes. *Deep-Sea Res. II* **45**, 2713–2737.

Cullen J. T., Chase Z., Coale K. H., Fitzwater S. E., and Sherrell R. M. (2003) Effect of iron limitation on the cadmium to phosphorus ratio on natural phytoplankton assemblages from the Southern Ocean. *Limnol. Oceanogr.* **48**, 1079–1087.

de Baar H. J. W., Croot P. L., Stoll M. H. C., Kattner G., Pickmere S., Freyer U., Boyd P., and Smetacek V. (2000) Nutrient anomalies of *Fragilariopsis kerguelensis* blooms revisited. Abstract Southern Ocean JGOFS Symposium, Brest, July 2000.

Donat J. R. and Bruland K. W. (1990) A comparison of two voltammetric techniques for determining zinc speciation in northeast Pacific Ocean waters. *Mar. Chem.* **28**, 301–323.

Donat J. R. and Bruland K. W. (1995) Trace elements in the oceans. In *Trace Elements in Natural Waters* (eds. E. Steinnes and B. Salbu). CRC Press, Boca Raton, FL, pp. 247–280.

Donat J. R. and van den Berg C. M. G. (1992) A new cathodic stripping voltammetric method for determining organic complexation of copper in seawater. *Mar. Chem.* **38**, 69–90.

Duce R. A. and Tindale N. W. (1991) Atmospheric transport of iron and its deposition on the ocean. *Limnol. Oceanogr.* **36**, 1715–1726.

Edmond J. M., Boyle E. A., Drummond D., Grant B., and Mislick T. (1978) Desorption of barium in the plume of the Zaire (Congo) River. *Netherlands J. Sea Res.* **12**, 324–328.

Edmond J. M., Measures C. I., Mangum B., Grant B., Sclater F. R., Collier R., Hudson A., Gordon L. I., and Corliss J. B. (1979) Formation of metal-rich deposits at ridge crests. *Earth Planet. Sci. Lett.* **46**, 19–30.

Elderfield H., Luedke N., McCaffery R. J., and Bender M. (1981) Benthic flux studies in Narragansett Bay. *Am. J. Sci.* **281**, 768–787.

Ellwood M. J. and van den Berg C. M. G. (2000) Zinc speciation in the Northeastern Atlantic Ocean. *Mar. Chem.* **68**, 295–306.

Ellwood M. J. and van den Berg C. M. G. (2001) Determination of organic complexation of cobalt in seawater by cathodic stripping voltammetry. *Mar. Chem.* **75**, 49–68.

Emerson S. R. and Huested S. S. (1991) Ocean anoxia and the concentration of molybdenum and vanadium in seawater. *Mar. Chem.* **34**, 177–196.

Falkowski P. G. (2000) Rationalizing elemental ratios in unicellular algae. *J. Phycol.* **36**, 3–6.

Flegal A. R. and Patterson C. C. (1983) Vertical concentration profiles of lead in the central Pacific at 15° N and 20° S. *Earth Planet. Sci. Lett.* **64**, 19–32.

Froelich P. N. and Andreae M. O. (1981) The marine geochemistry of germanium: Ekasilicon. *Science* **213**, 205–207.

Goldberg E. D. (1954) Marine Geochemistry: 1. Chemical scavengers of the sea. *J. Geol.* **62**, 249–265.

Hering J. G. and Morel F. M. M. (1990) Kinetics of trace-metal complexation-ligand-exchange reactions. *Environ. Sci. Technol.* **24**, 242–252.

Hunter K. A., Kim J. P., and Croot P. L. (1997) Biological role of trace metals in natural waters. *Environ. Monitor. Assess.* **44**, 103–147.

Hutchins D. A. and Bruland K. W. (1994) Grazer-mediated regeneration and assimilation of Fe, Zn, and Mn from planktonic prey. *Mar. Ecol. Prog. Ser.* **11**, 259–269.

Hutchins D. A. and Bruland K. W. (1995) Fe, Zn, Mn and N transfer between size classes in a coastal phytoplankton community: trace metal and major nutrient recycling compared. *J. Mar. Res.* **53**, 1–18.

Hutchins D. A. and Bruland K. W. (1998) Iron-limited diatom growth and Si : N uptake in a coastal upwelling regime. *Nature* **393**, 561–564.

Hutchins D. A., DiTullio G. R., and Bruland K. W. (1993) Iron and regenerated production: evidence for biological iron recycling. *Limnol. Oceanogr.* **38**, 1242–1255.

Hutchins D. A., Witter A. E., Butler A., and Luther G. W. (1999) Competition among marine phytoplankton for different chelated iron species. *Nature* **400**, 858–861.

Hydes D. J. (1979) Aluminum in seawater: control by inorganic processes. *Science* **205**, 1260–1262.

Hydes D. J. (1983) Distribution of aluminum in waters of the Northeast Atlantic 25-degrees-N to 35-degrees-N. *Geochim. Cosmochim. Acta* **47**, 967–973.

Hydes D. J., De Lange G. T., and De Baar H. J. W. (1988) Dissolved aluminum in the Mediterranean. *Geochim. Cosmochim. Acta* **52**, 2107–2114.

Jickells T. M. (1995) Atmospheric inputs of metals and nutrients to oceans: their magnitude and effects. *Mar. Chem.* **48**, 199–214.

Jickells T. M. and Spokes L. J. (2001) Atmospheric iron inputs to the oceans. In *The Biogeochemistry of Iron in Seawater* (eds. D. R. Turner and K. Hunter). Wiley, Chichester, pp. 85–121.

Johnson K. S., Gordon R. M., and Coale K. H. (1997) What controls dissolved iron concentrations in the world ocean? *Mar. Chem.* **57**, 137–161.

Johnson K. S., Chavez F. P., and Friederich G. E. (1999) Continental-shelf sediments as a primary source of iron for coastal phytoplankton. *Nature* **398**, 697–700.

Karl D. M. (2002) Nutrient dynamics in the deep blue sea. *Trends Microbiol.* **10**, 410–418.

Kim J. P., Hunter K. A., and Reid M. R. (1999) Geochemical processes affecting the major ion composition of river in the South Island, New Zealand. *Mar. Freshwater Res.* **50**, 699–707.

Lee J. G. and Morel F. M. M. (1995) Replacement of zinc by cadmium in marine phytoplankton. *Mar. Ecol. Prog. Ser.* **127**, 305–309.

Lewis B. L., Froelich P. N., and Andreae M. O. (1985) Methylgermanium in natural waters. *Nature* **313**, 303–305.

Lewis B. L., Andreae M. O., and Froelich P. N. (1989) Sources and sinks of methylgermanium in natural waters. *Mar. Chem.* **27**, 179–200.

Liu X. W. and Millero F. J. (2002) The solubility of iron in seawater. *Mar. Chem.* **77**, 43–54.

Lohan M. C., Statham P. J., and Crawford D. W. (2002) Dissolved zinc in the upper water column of the subarctic North East Pacific. *Deep-Sea Res. II* **49**, 5793–5808.

Macrellis H. M., Trick C. G., Rue E. L., Smith G. J., and Bruland K. W. (2001) Collection and detection of natural iron-binding ligands from seawater. *Mar. Chem.* **76**, 175–187.

Maldonado M. T. and Price N. M. (1999) Utilization of iron bound to strong organic ligands by plankton communities in the subarctic Pacific Ocean. *Deep-Sea Res. II* **46**, 2447–2473.

Mahowald N., Kohfeld K., Hannson M., Balkanski Y., Harrison S. P., Prentice I. C., Schulz M., and Rodhe H. (1999) Dust sources during the last glacial maximum and current climate: a comparison of model results with paleodata from ice cores and marine sediments. *J. Geophys. Res.* **104**, 15895–15916.

Marchitto T. M., Oppo D. W., and Curry W. B. (2002) Paired benthic foraminiferal Cd/Ca and Zn/Ca evidence for a greatly increased presence of Southern Ocean Water in the glacial North Atlantic. *Paleoceanography* **17**, 1038.

Martin J. H. and Gordon R. M. (1988) Northeast Pacific iron distributions in relation to phytoplankton productivity. *Deep-Sea Res.* **35**, 177–196.

Martin J. H. and Knauer G. A. (1973) The elemental composition of plankton. *Geochim. Cosmochim. Acta* **37**, 1639–1653.

Martin J., Bruland K. W., and Broenkow W. (1976) Cadmium transport in the California current. In *Marine Pollutant Transfer* (eds. H. L. Windom and R. A. Duce). Lexington Books, Toronto, pp. 84–159.

Martin J. H., Knauer G. A., and Gordon R. M. (1983) Silver distributions and fluxes in the North-east Pacific waters. *Nature* **305**, 306–309.

Martin J. H., Gordon R. M., Fitzwater S., and Broenkow W. W. (1989) VERTEX: phytoplankton/iron studies in the Gulf of Alaska. *Deep-Sea Res.* **36**, 649–680.

Martin J. H., Fitzwater S. E., Gordon R. M., Hunter C. N., and Tanner S. J. (1993) Iron, primary production and carbon–nitrogen flux studies during the JGOFS North Atlantic Bloom Experiment. *Deep-Sea Res.* **40**, 115–134.

Martin J. H., Coale K. H., Johnson K. S., Fitzwater S. E., Gordon R. M., Tanner S. J., Hunter C. N., Elrod V. A., Nowicki J. L., Coley T. L., Barber R. T., Lindley S., Watson A. J., Vanscoy K., Law C. S., Liddicoat M. I., Ling R., Stanton T., Stockel J., Collins C., Anderson A., Bidigare R., Ondrusek M., Latasa M., Millero F. J., Lee K., Yao W., Zhang J. Z., Friederich G., Sakamoto C., Chavez F., Buck K., Kolber Z., Greene R., Falkowski P., Chisholm S. W., Hoge F., Swift R., Yungel J., Turner S., Nightingale P., Hatton A., Liss P., and Tindale N. W. (1994) Testing the iron hypothesis in ecosystems of the equatorial Pacific-Ocean. *Nature* **371**, 123–129.

Measures C. I. and Brown E. T. (1996) Estimating dust input to the Atlantic Ocean using surface water Al concentrations. In *The Impact of African Dust across the Mediterranean* (eds. S. Guerzoni and R. Chester). Kluwer, Dordrecht, 398pp.

Measures C. I. and Edmond J. M. (1982) Beryllium in the water column of the central North Pacific. *Nature* **257**, 51–53.

Measures C. I., Yuan J., and Resing J. A. (1995) Determination of iron in seawater by flow injection-analysis using in-line preconcentration and spectrophotometric detection. *Mar. Chem.* **50**, 3–12.

Moffett J. W. and Brand L. E. (1996) Production of strong, extracellular Cu chelators by marine cyanobacteria in response to Cu stress. *Limnol. Oceanogr.* **41**, 388–395.

Moffett J. W., Brand L. E., and Zika R. G. (1990) Distribution and potential sources and sinks of copper chelators in the Sargasso Sea. *Deep-Sea Res.* **37**, 27–36.

Moore J. K., Doney S. C., Glover D. M., and Fung I. Y. (2002) Iron cycling and nutrient limitation patterns in surface waters of the world ocean. *Deep-Sea Res. II* **49**, 463–507.

Morel F. M. M., Reuter J., Anderson D., and Guillard R. (1979) Aquil: a chemically defined phytoplankton culture medium for trace metal studies. *Limnol. Oceanogr.* **36**, 27–36.

Morford J. L. and Emerson S. S. (1999) The geochemistry of redox sensitive trace metals in sediments. *Geochim. Cosmochim. Acta* **63**, 1735–1750.

Morley N. H., Statham P. J., and Burton J. D. (1993) Dissolved trace metals in the southwestern Indian Ocean. *Deep-Sea Res.* **30**, 1043–1062.

Murname R. J. (1994) Determination of thorium and particulate matter cycling parameters at Station P: a reanalysis and comparison of least squares techniques. *J. Geophys. Res.* **99**, 3393–3405.

Nozaki Y., Yang H. S., and Yamada M. (1987) Scavenging of thorium in the ocean. *J. Geophys. Res.* **92**, 772–778.

Nriagu J. (1989) The rise and fall of leaded gasoline. *Sci. Total Environ.* **92**, 13–28.

Orians K. J. and Bruland K. W. (1985) Dissolved aluminum in the central North Pacific. *Nature* **316**, 427–429.

Orians K. J. and Bruland K. W. (1986) The biogeochemistry of aluminum in the Pacific Ocean. *Earth Planet. Sci. Lett.* **78**, 397–410.

Orians K. J. and Bruland K. W. (1988) The marine geochemistry of dissolved gallium: a comparison with dissolved aluminum. *Geochim. Cosmochim. Acta* **52**, 1–8.

Powell R. T. and Donat J. R. (2001) Organic complexation and speciation of iron in the South and equatorial Atlantic. *Deep-Sea Res. II* **48**, 2877–2893.

Price N. M. and Morel F. M. M. (1990) Cadmium and cobalt substitution for zinc in a marine diatom. *Nature* **344**, 658–660.

Price N. M., Harrison G. I., Hering J. G., Hudson R. J., Nirel P., Palenik B., and Morel F. M. M. (1988/89) Preparation and chemistry of the artifical algal culture medium Aquil. *Biol. Oceanogr.* **5**, 43–46.

Rivera-Duarte I., Flegal A. R., Sanudo-Wilhelmy S. A., and Veron A. J. (1999) Silver in the far North Atlantic Ocean. *Deep-Sea Res. II* **46**, 979–990.

Roy-Barman M., Chen J. H., and Wasserburg G. J. (1996) ^{230}Th–^{232}Th systematics in the central Pacific Ocean: the sources and fates of thorium. *Earth Planet. Sci. Lett.* **139**, 315–363.

Rue E. L. and Bruland K. W. (1995) Complexation of iron(III) by natural organic ligands in the central North Pacific as determined by a new competitive ligand equilibration/ adsorptive cathodic stripping voltammetry method. *Mar. Chem.* **50**, 117–138.

Rue E. L. and Bruland K. W. (1997) The role of organic complexation on ambient iron chemistry in the equatorial Pacific Ocean and the response of a mesoscale iron addition experiment. *Limnol. Oceanogr.* **42**, 901–910.

Saito M. A. and Moffett J. W. (2001) Complexation of cobalt by natural organic ligands in the Sargasso Sea as determined by a new high-sensitivity electrochemical cobalt speciation method suitable for open ocean work. *Mar. Chem.* **75**, 69–88.

Schaule B. K. and Patterson C. C. (1981) Lead concentrations in the northeast Pacific: evidence for global anthropogenic perturbations. *Earth Planet. Sci. Lett.* **54**, 97–116.

Schaule B. K. and Patterson C. C. (1983) Perturbations of the natural lead depth profile in the Sargasso Sea by industrial lead. In *Trace Metals in Seawater* (eds. C. S. Wong, E. Boyle, K. W. Bruland, J. D. Burton, and E. D. Goldberg). Plenum, New York, pp. 487–503.

Shiller A. M. and Boyle E. A. (1991) Trace elements in the Mississippi river-delta outflow region-behaviour at high discharge. *Geochim. Cosmochim. Acta* **55**, 3241–3251.

Sholkovitz E. R. and Copeland D. (1983) The coagulation, solubility and adsorption properties of Fe, Mn, Cu, Ni, Cd, Co and humic acids in river water. *Geochim. Cosmochim. Acta* **45**, 181–189.

Smetacek V. (1999) Diatoms and the ocean carbon cycle. *Protist* **150**, 25–32.

Sohrin Y., Isshiki K., Nakayama E., and Matsui M. (1989) Simultaneous determination of tungsten and molybdenum in sea-water by catalytic current polarography after pre-concentration on a resin column. *Anal. Chim. A* **218**, 25–35.

Spencer D. W., Robertson D. E., Turekian K. K., and Folsom T. M. (1970) Trace element calibrations and profiles at the GEOSECS test station in the northeast Pacific Ocean. *J. Geophys. Res.* **75**, 7688.

Sunda W. G. (1988/89) Trace metal interactions with marine phytoplankton. *Biol. Oceanogr.* **6**, 411–442.

Sunda W. G. and Huntsman S. A. (1992) Feedback interactions between zinc and phytoplankton in seawater. *Limnol. Oceanogr.* **37**, 25–40.

Sunda W. G. and Huntsman S. A. (1995a) Iron uptake and growth limitation in oceanic and coastal phytoplankton. *Mar. Chem.* **50**, 189–206.

Sunda W. G. and Huntsman S. A. (1995b) Cobalt and zinc interreplacement in marine phytoplankton: biological and geochemical implications. *Limnol. Oceanogr.* **40**, 1404–1407.

Sunda W. G. and Huntsman S. A. (1995c) Regulation of copper concentration in the oceanic nutricline by phytoplankton uptake and regeneration cycles. *Limnol. Oceanogr.* **40**, 132–137.

Sunda W. G. and Huntsman S. A. (1998) Control of Cd concentrations in a coastal diatom by interactions among free ionic Cd, Zn, and Mn in seawater. *Environ. Sci. Technol.* **32**, 2961–2968.

Takeda S. (1998) Influence of iron availability on nutrient consumption ratio of diatoms in oceanic waters. *Nature* **393**, 774–777.

Tappin A. D., Millward G. E., Statham P. J., Burton J. D., and Morris A. W. (1995) Trace metal in the central and southern North Sea. *Estuar. Coast. Shelf Sci.* **41**, 275–323.

Tegen I. and Fung I. (1995) Contribution to the atmospheric mineral aerosol load from land-surface modification. *J. Geophys. Res.* **100**, 18707–18726.

Turekian K. K. (1977) The fate of metals in the oceans. *Geochim. Cosmochim. Acta* **41**, 1139–1144.

Turner D. R., Whitfield M., and Dickson A. G. (1981) The equilibrium speciation of dissolved components in freshwater and seawater at 25 °C and 1 atm pressure. *Geochim. Cosmochim. Acta* **45**, 855–881.

van den Berg C. M. G. (1984) Determination of copper in seawater by cathodic stripping voltammetry of complexes with catechol. *Anal. Chim. A* **164**, 195–207.

van den Berg C. M. G. (1985) Determination of the zinc complexing capacity in seawater by cathodic stripping voltammetry of zinc-APDC complex ions. *Mar. Chem.* **16**, 121–130.

van den Berg C. M. G. (1988) Adsorptive cathodic stripping voltammetry and chronopotentiometry of trace metals in sea water. *Anal. Proc.* **25**, 265–266.

van den Berg C. M. G. (1995) Evidence for organic complexation of iron in seawater. *Mar. Chem.* **50**, 139–157.

Vink S. and Measures C. I. (2001) The role of dust deposition in determining surface water distributions of Al and Fe in the South west Atlantic. *Deep-Sea Res.* **48**, 2787–2809.

von Damm K. L., Edmond J. M., Measures C. L., and Grant B. (1985) Chemistry of submarine hydrothermal solutions at 21° N, East Pacific Rise. *Geochim. Cosmochim. Acta* **49**, 2197–2220.

Vorlicek T. P. and Helz G. R. (2002) Catalysis by mineral surfaces: implications for Mo geochemistry in anoxic environments. *Geochim. Cosmochim. Acta* **66**, 3679–3692.

Westerlund S. F. G., Anderson L. G., Hall P. O. J., Iverfeldt A., Vanderloff M. M. R., and Sundby B. (1986) Benthic flues of cadmium, copper, nickel and lead in coastal environments. *Geochim. Cosmochim. Acta* **50**, 1289–1296.

Wilhelm S. W. and Trick C. G. (1994) Iron-limited growth of cyanobacteria: multiple siderophore production is a common response. *Limnol. Oceanogr.* **39**, 197–1984.

Windom H., Byrd J., Smith R., Hungspreugs M., Dharmvanii S., Thumtrakul W., and Yeats P. (1991) Trace-metal nutrients relationships in estuaries. *Mar. Chem.* **32**, 177–194.

Wu J. and Boyle E. A. (1997) Low blank preconcentration technique for the determination of lead, copper and cadmium in small-volume seawater samples by isotope dilution ICPMS. *Anal. Chem.* **69**, 2464–2470.

Wu J. F. and Luther G. W. (1995) Complexation of Fe(III) by natural organic ligands in the northwest Atlantic Ocean by a competitive ligand equilibration method and a kinetic approach. *Mar. Chem.* **50**, 159–177.

Zhang Y., Amakawa H., and Nozaki Y. (2001) Oceanic profiles of dissolved silver; precise measurements in the basins of western North Pacific, Sea of Okhotsk, and the Japan Sea. *Mar. Chem.* **75**, 151–162.

Zhu X. R., Prospero J. M., and Millero F. J. (1997) Diel variability of soluble Fe(II) and soluble total Fe in North African dust in the trade winds near Barbados. *J. Geophys. Res.* **102**, 21297–21305.

Treatise on Geochemistry
ISBN (set): 0-08-043751-6

Volume 6; (ISBN: 0-08-044341-9); pp. 23–47